nature chemical biology

Article

https://doi.org/10.1038/s41589-026-02230-0

H_2O_2-free proximity proteomics for exploring dynamic protein complexes in living systems

Received: 9 May 2025

Accepted: 22 April 2026

Published online: 28 May 2026

Check for updates

Mi Ke[1,7], Fuchao Liang[1,7], Guangqin Wang[2,7], An He[1,7], Baixu Ma[1], Zheyi Liu[3], Jie Wang[1], Yan Xu[4], Yanli Li[4], Zhe Dong[1], Zhihua Zhong[1], Zhiyao Tang[1], Pengyu Sun[5,6], Kangmin He[5,6], Fangjun Wang[3], Zhiyong Liu[2] ✉, Xueming Yang[1], Lizhi Tao[1] ✉ & Ruijun Tian[1] ✉

Dynamic protein complex assembly is critical for regulating various biological processes. Proximity labeling (PL), best represented by the ascorbate peroxidase APEX2, allows these molecular events to be captured in living cells in a spatiotemporal manner. However, the hydrogen peroxide (H_2O_2) dependence of APEX2 has hindered its application in sensitive living systems. Here we introduce ROProx, a radical- and oxygen-driven photoreactive PL technology that leverages the chemically evolved biotin-naphthylamine probe BN2, which has strong binding affinity for APEX2, and the unexpected tyrosyl radicals in APEX2. ROProx labels dynamic cytosolic protein complexes in living cells within seconds, with a range of 10 nm, and is precisely controlled by mild blue light irradiation without H_2O_2. Additionally, we apply ROProx to explore the phosphotyrosine-dependent GRB2 interactome in living mice by simply injecting BN2 for 5 minutes. ROProx should, therefore, open broad opportunities for PL chemical evolution and applications in other living systems.

Proteins are fundamental building blocks of life, as cellular processes are largely governed by well-organized protein assemblies[1]. These protein machineries range from static to dynamically assembled protein complexes, which are often modulated by posttranslational modifications[2]. The best example of such complexes are those mediated by phosphotyrosine (pTyr), which are spatiotemporally regulated within minutes or even seconds and sophisticatedly organized by scaffolding proteins carrying pTyr-binding domains[3,4]. Dynamic changes in pTyr protein complexes in response to different stimuli, such as secreted ligands and cell–cell interactions, have been integrated into various signaling networks, especially in the immunological microenvironment[3,5]. More importantly, the continuously increasing number of FDA-approved kinase inhibitors[6] and immune checkpoint therapies[7] underscores the importance of pTyr-mediated signal transduction in targeted therapies. However, efficiently capturing these dynamic signaling events in their native biological system remains a major technical challenge.

PL combined with mass spectrometry (MS)-based proteomics enables the precise capture and identification of proteins that are closely associated with a target protein in living cells. Among these

[1]State Key Laboratory of Medical Proteomics and Shenzhen Key Laboratory of Functional Proteomics, Department of Chemistry and Research Center for Chemical Biology and Omics Analysis, College of Science and Guangming Advanced Research Institute, Southern University of Science and Technology, Shenzhen, China. [2]Institute of Neuroscience, State Key Laboratory of Neuroscience, CAS Center for Excellence in Brain Science and Intelligence Technology, Chinese Academy of Sciences, Shanghai, China. [3]Dalian Institute of Chemical Physics, Chinese Academy of Sciences, Dalian, China. [4]Biotherapy Centre, The Third Affiliated Hospital of Sun Yat-sen University, Guangzhou, China. [5]Institute of Genetics and Developmental Biology, Chinese Academy of Sciences, Beijing, China. [6]University of Chinese Academy of Sciences, Beijing, China. [7]These authors contributed equally: Mi Ke, Fuchao Liang, Guangqin Wang, An He. ✉e-mail: zhiyongliu@ion.ac.cn; taolz@sustech.edu.cn; tianrj@sustech.edu.cn

https://doi.org/10.1038/s41589-026-02230-0

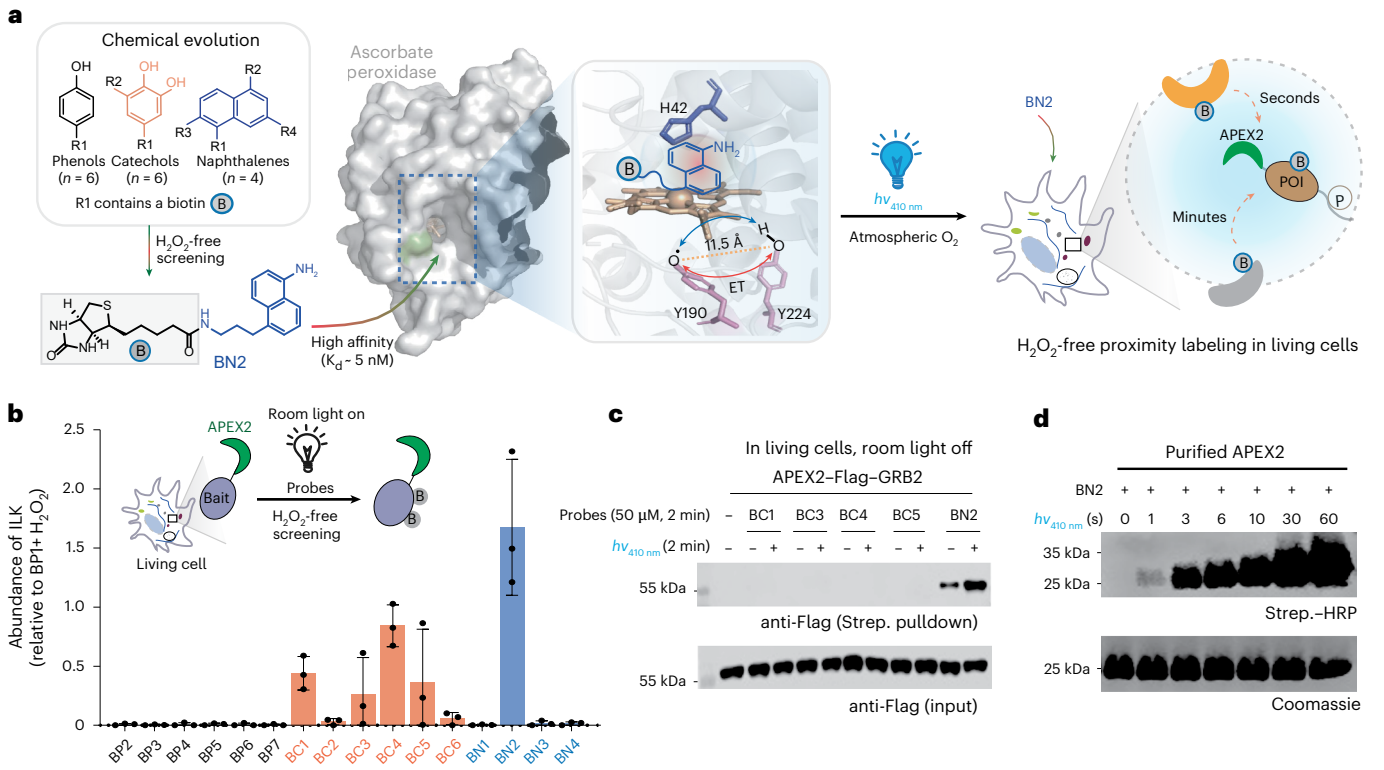

Fig. 1 | Development of the H_2O_2-free photoreactive PL technology ROProx. **a**, Left, chemical evolution explored BN2 with high affinity to APEX2 and BN2-based H_2O_2-free PL. Crystal structure and EPR analysis revealed stable tyrosine-phenoxyl radical-based photoreactive PL. Right, ROProx achieved second-scale PL in living cells in the presence of 410-nm mild blue light. **b**, Quantification of the labeling activity of the 16 BP analogs. Streptavidin pulldown of ILK was quantified and normalized to input ILK. BP1 with 500 μM H_2O_2 was used as a positive control to calculate labeling efficiency (biological replicates $n = 3$); data are presented as mean values ± s.e.m. **c**, Photoreactivity test of the five probes that show H_2O_2-independent labeling capability (biological replicates $n = 3$). **d**, BN2 labeling of purified APEX2 in vitro induced by second-scale resolution of blue light exposure (biological replicates $n = 3$). Strep., streptavidin.

methods, BioID[8] has been widely used for studying subcellular proteomes[9] and stable protein complexes[10] in living cells. However, the BioID requirement of extended labeling duration limits its utility for analyzing dynamic protein assemblies[8,11]. Although the TurboID variant of BioID has shown improved labeling efficiency and a reduced labeling duration of 10 minutes, it is still not suitable for studying rapid protein dynamics[12,13]. Recent advances in photoreactive enzyme (PRE)-mediated labeling technologies, including SOPP3–APEX2 (ref. 14), miniSOG[15], LOV-Turbo[16] and LITag[17], use visible light activation to control the PL processes on the order of seconds. However, these methods still face limitations, such as the limited penetration of light into living animals[17]. APEX2, which evolved from the pea ascorbate peroxidase APX[18], is a popular PL enzyme suitable for spatiotemporal protein complex profiling, such as for GPCR-associated complexes, which dynamically assemble within seconds[19,20]. To improve the labeling selectivity of APEX2, we identified the substrate probes BP5 and BN2, which have self-quenching properties via polymerization and outperform biotin-phenol for labeling dynamic protein complexes, especially those without a defined cellular localization[21]. However, the reliance of APEX2 on H_2O_2 limits its application for studying dynamic processes in living systems[22] and H_2O_2-sensitive signaling pathways[23]. These challenges underscore the need for new PL technologies with improved kinetics, selectivity and biocompatibility to advance the study of dynamic protein assemblies in vivo.

To address these challenges, we developed the ROProx system, which integrates exogenous H_2O_2-free and photoreactive labeling while retaining the rapid kinetics of APEX2-mediated PL. We identified BN2 from the chemical evolution of 16 rationally designed and synthesized candidate probes as a highly efficient and selective probe capable of labeling dynamic protein complexes in an APEX2-dependent and dual-modal manner. BN2 represents a major advancement in PL methodology in two key aspects. In the first mode, it enables highly selective photoreactive labeling of protein complexes within a confined 10-nm radius in living cells within seconds, driven by its high binding affinity for APEX2 and the tyrosyl radicals of APEX2. Notably, the labeling reaction preferentially targets histidine residues rather than tyrosine and is precisely regulated by atmospheric O_2 and mild blue light irradiation. Furthermore, this BN2–APEX2-dependent PL approach operates entirely without H_2O_2, making it particularly suitable for use in H_2O_2-sensitive biological systems. Crucially, high labeling selectivity is achieved through a unique dual-brake mechanism, involving site-specific labeling of BN2 to the His42 residue of APEX2 and self-quenching via BN2 polymerization. In the second mode, ROProx is responsive to extremely low levels of H_2O_2 and favors to label tyrosine residues[21], which is well suitable for in vivo applications, as we demonstrated for dynamic interactome profiling in live animal models. Collectively, the finely tuned labeling performance offered by ROProx holds broad potential for applications across diverse living cells and in vivo systems.

Results

Development of an H_2O_2-free ROProx system that is photoreactive

To identify PL chemical probes that use APEX2 but independent of H_2O_2, we designed and synthesized 16 chemical probes that fall into three structurally diverse categories (Fig. 1a and Extended Data Fig. 1a): (1) six biotin-phenol (BP) derivatives, which are commonly used in peroxidase-based PL applications[21,24]; (2) six catechol-based (BC) probes;

and (3) four aniline-functionalized or naphthalene-functionalized (BN) compounds. Among them, seven of these chemical probes were newly designed and synthesized (Supplementary Figs. 1–9). This collection served as the foundation for the development of chemical PL probes for exogenous H_2O_2-free PL. To evaluate H_2O_2-independent PL, we incubated each chemical probe for 10 minutes with a cell line expressing ILK fused to APEX2–Flag at its N terminus. The labeling performance of the bait protein ILK was then assessed via pulldown assays followed by western blotting. Labeling intensities were quantified based on the amount of ILK recovered from streptavidin pulldown, normalized to a positive control using the well-established BP1 probe in combination with H_2O_2 (Fig. 1b). Among the tested probes, BN2, BC1, BC3, BC4 and BC5 exhibited robust labeling activity in the absence of exogenous H_2O_2. Notably, all five probes share catechol-derived or naphthalene-derived structural features, suggesting a distinct mode of chemical reactivity compared to traditional BP-based probes. Further experiments involving H_2O_2 treatment and extended incubation (up to 60 minutes) confirmed that the labeling performance of these five probes was largely independent of exogenous H_2O_2 (Extended Data Fig. 1b,c). Among them, BN2 demonstrated the highest labeling efficiency, which was unexpected because we previously discovered that BN2 is a highly selective APEX2-dependent PL chemical probe in the presence of 500 µM H_2O_2 for 1 minute[21].

To investigate the underlying mechanism of BN2-mediated, H_2O_2-free labeling and inspired by recent advances in visible light-activated chemical and enzymatic PL systems[17,25,26], we hypothesized that the labeling process might be triggered either by endogenous H_2O_2 within living cells or by visible light emitted from room light. Considering that APEX2 exhibits a Soret maximum at 410 nm from the high-spin ferric heme (Extended Data Fig. 1d)[27], we sought to distinguish between these two potential effectors. We conducted experiments using a cell line expressing growth factor receptor-bound protein 2 (GRB2) tagged with APEX2–Flag, incubated with BN2 either in complete darkness or under brief exposure to 410-nm blue light for 2 minutes (Extended Data Fig. 1e). Notably, a marked increase in labeling intensity was observed upon light exposure compared to the group incubated with BN2 in the dark, indicating that blue light primarily drives the labeling reaction, whereas endogenous H_2O_2 contributes only a minimal baseline activity. Additionally, BC1, BC3, BC4 and BC5 were also tested for their photoreactivity under 410-nm blue light for 2 minutes; however, none of the four probes exhibited any photoreactivity (Fig. 1c). To assess wavelength dependence, we exposed the BN2–APEX2 system to various wavelengths, including ultraviolet, blue, green and red light. Among these, the highest labeling efficiency was observed under 410-nm irradiation at an intensity of 34 mW cm^{-2} (Extended Data Fig. 1f). Notably, BN2 combined with purified APEX2 enabled robust protein labeling after just 3 seconds of light exposure (Fig. 1d), a result that was also observed in living cells (Extended Data Fig. 1g). These findings indicate that BN2 and blue light not only enable a robust labeling efficiency without H_2O_2 but also markedly accelerate the reaction kinetics to the timescale of seconds. Thus, through chemical screening, we identified BN2 as a synergistic probe for APEX2 and developed an H_2O_2-free, photoreactive PL technology, which we termed ROProx.

Unique molecular mechanisms advance the photoreactive PL

To understand the mechanism of the ROProx system from a molecular perspective, we determined the first X-ray crystal structure of APEX2 (Protein Data Bank (PDB): 9KOE; Supplementary Table 1). Notably, we found that the photoreactivity of ROProx was strictly dependent on the simultaneous presence of BN2, APEX2 and blue light, underscoring its unique, highly specific activation mechanism (Fig. 2a). The data above also suggest a unique interaction between BN2 and APEX2 that advances photoreactivity. To further investigate this interaction, we performed biolayer interferometry (BLI), which revealed high-affinity binding between BN2 and purified APEX2 with $K_d \approx 4.95$ nM. This binding was markedly stronger than other combinations, such as BP1–APEX2 ($K_d \approx 528$ nM) and BN2–HRP ($K_d \approx 6220$ nM) (Fig. 2b and Supplementary Table 1). Notably, too, neither the BP1–APEX2 nor the BN2–HRP combinations exhibited in vitro photoreactivity like the BN2–APEX2 combination (Fig. 2c). Furthermore, ultraviolet photodissociation (UVPD, 193 nm) native top-down MS was employed to confirm the BN2–APEX2 interaction. The MS1 spectra revealed multiple charge states (9+, 10+ and 11+) of the APEX2 (apo)–heme–BN2 ternary complex (Extended Data Fig. 2a, left). UVPD tandem MS analysis of the 10+ charge state identified distinct ions, including BN2–heme and APEX2 fragments (Extended Data Fig. 2a, right). Fragment mapping revealed three regions in APEX2 strongly affected by BN2 binding (Extended Data Fig. 2b and Supplementary Table 2), among which residues 69–78, located near the heme cofactor, were particularly notable. Notably, too, no structural obstruction was observed between this region and the heme, underscoring its accessibility for BN2 binding. These findings collectively advance our understanding of the structural determinants underlying the role of BN2 in ROProx technology. Further structural analysis highlighted that the H169 residue in APEX2 regulated the access or binding of BN2 to APEX2 through the exposed heme edge (Extended Data Fig. 2c)[28]. This conclusion was supported by experiments on the H169A mutant, which showed a notably reduced affinity for BN2 compared to wild-type APEX2 (Fig. 2b). Additionally, the complete loss of photoreactivity in the H169A mutant (Fig. 2d) further reinforces this finding. Therefore, we conclude that the strong binding affinity between BN2 and APEX2 is essential for the photoreactive labeling.

As both APEX2 and HRP enzymes are heme-cofactor-containing metallo-peroxidases, we employed electron paramagnetic resonance (EPR) spectroscopy to characterize any paramagnetic species involved in the ROProx process. Both the as-purified APEX2 and HRP exhibit high-spin ferric heme species ($S = 5/2$) with characteristic g-values around 6.0, as observed from the EPR spectra at 10 K (Fig. 2e, left, and Supplementary Table 3)[29]. Additionally, APEX2 harbors a distinct radical signal with g-value ≈ 2.0, which can be clearly observed at 50 K due to its slower relaxation property compared to high-spin ferric heme (Fig. 2e, right). Although a similar radical was also shown in the original APX, no radical signal was detected in HRP. Further experiments incubating APEX2 with BN2 revealed that exposure to blue light (410 nm) notably increased the formation of radical species under aerobic conditions (Fig. 2f and Extended Data Fig. 2d). By contrast, the BP1 probe did not show any enhancement of radical signals under the same conditions (Fig. 2g and Extended Data Fig. 2e). In addition, EPR experiments using H169A incubated with BN2 showed no radical signal enhancement when exposed to blue light either (Extended Data Fig. 2f). This suggests that the binding of BN2 to the enzyme is crucial. Interestingly, BN2 bound APX with affinity similar to APEX2 (Fig. 2b) but exhibited much weaker photoreactive labeling activity (Extended Data Fig. 2g). In addition, no increase in tyrosyl radical signals was detected when APX–BN2 was exposed to blue light (Extended Data Fig. 2h).

We continued to analyze the EPR signal (Fig. 2h, black trace), which shows that the radical signal in APEX2 consists of two species. One species that is retained after the addition of BN2 (Fig. 2h, blue trace) shows the g-values of [2.0060, 2.0040, 2.0030] with $g_{iso} = 2.0043$, typical for a tyrosyl radical (Supplementary Table 2), although the g anisotropy is slightly small. Q-band pulse ^{1}H electron nuclear double resonance (ENDOR) spectra show the typical ^{1}H hyperfine coupling as assigned to ^1H7_a, ^{1}H5 and ^{1}H3, supporting the tyrosyl radical assignment (Extended Data Fig. 2i). The other species is more isotropic with g-value of 2.003, which is likely a non-oxygen-based radical[30]. It can be quenched by BN2, and the quenched radical may be related to the oxidation of BN2. Although the latter radical is also observed in other heme-cofactor-containing metallo-enzymes[30], the presence of the tyrosyl radical in the as-purified enzyme is notable, as no H_2O_2 was

https://doi.org/10.1038/s41589-026-02230-0

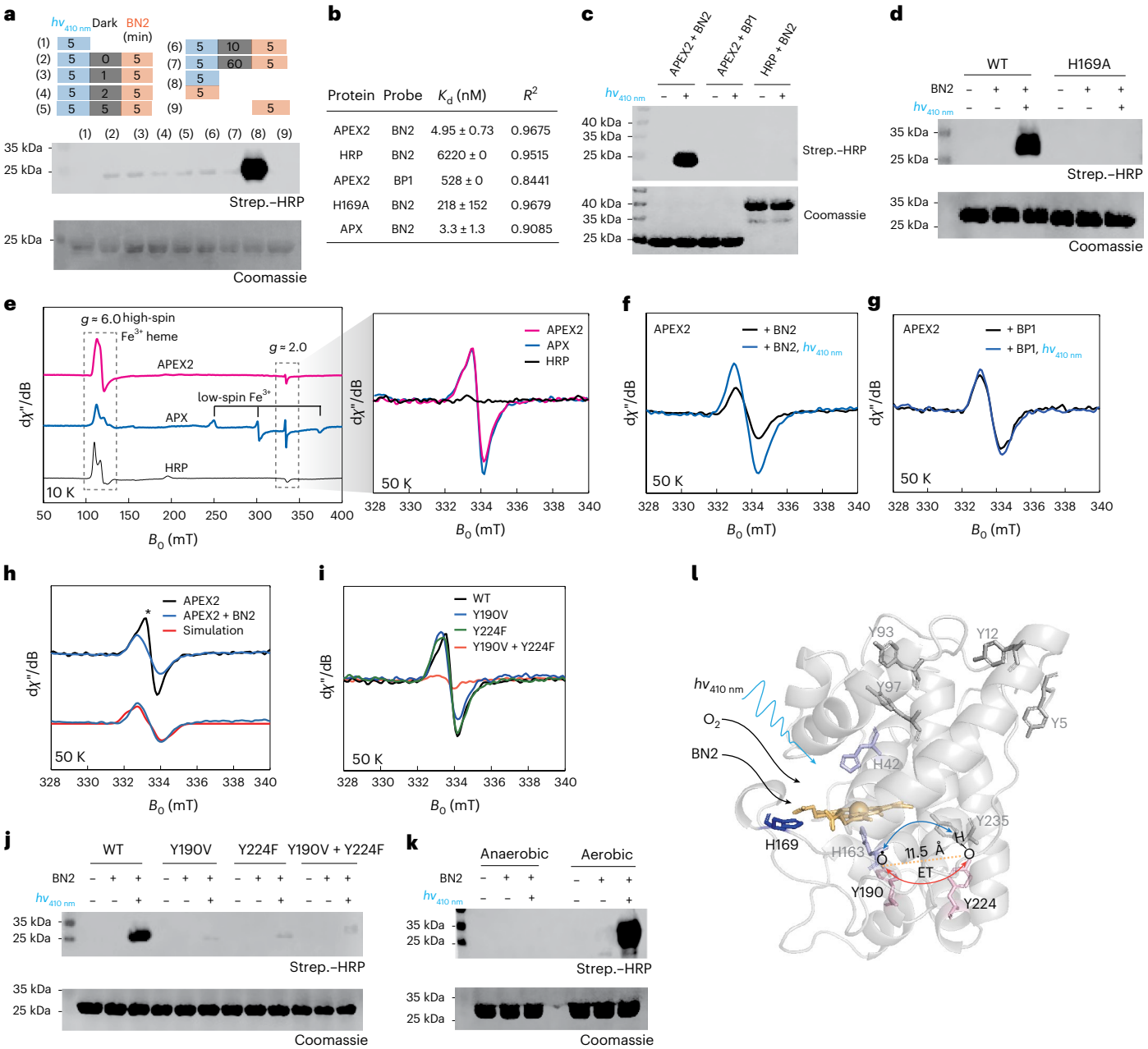

Fig. 2 | Molecular mechanisms of ROProx. a, Testing the dependency of ROProx-mediated PL on blue light, BN2 and APEX2 in vitro (biological replicates $n = 3$). **b**, BLI measurement of the affinity between BN2/BP1 and HRP/APEX2/H169A/APX (biological replicates $n = 3$). **c**, BN2/BP1 labeling of the peroxidases APEX2/HRP upon blue light exposure (biological replicates $n = 3$). **d**, Testing the photoreactivity of BN2 with wild-type APEX2 or H169A mutant after 2 minutes of blue light exposure (biological replicates $n = 3$). **e**, X-band CW EPR spectra of purified APEX2, APX and HRP. The purified APX also shows low-spin Fe^{3+} heme signal with the g-values of [2.675, 2.212, 1.783]. **f**, X-band CW EPR spectra (50 K) of the APEX2 radical signals upon BN2 treatment or blue light exposure under aerobic condition. The related full spectra at 10 K are shown in Extended Data Fig. 2d. **g**, X-band CW EPR spectra (50 K) of the APEX2 radical signals upon BP1 treatment or blue light exposure under aerobic condition. The related full spectra at 10 K are shown in Extended Data Fig. 2e. **h**, X-band CW EPR spectra (50 K) of purified APEX2 or APEX2 treated with equal molar of BN2. The asterisk (*) indicates the tyrosyl radical signal. **i**, X-band CW EPR spectra of APEX2 and varying tyrosine mutants at 50 K. The related full spectra at 10 K are shown in Extended Data Fig. 2n. **j**, Photoreactive activities of the tyrosine mutants were assessed. BN2 was 500 μM, and mutants were at 1 μg μl^{-1} and exposed to blue light for 5 minutes (biological replicates $n = 3$). **k**, Assessment of APEX2's photoreactivity with or without O_2 (biological replicates $n = 3$). **l**, Conclusion of the necessary factors for the H_2O_2-free reactivity of ROProx: (1) BN2; (2) blue light; (3) O_2; (4) the accessibility of BN2 into the pocket of APEX2 through H169 residue; and (5) the tyrosyl radical hops between Y190 and Y224 in APEX2. CW, continuous-wave; B_0, magnetic field; mT, millitesla; dχ''/dB, the derivative of the absorption signal with respect to the external static magnetic field in arbitrary units; Strep., streptavidin; WT, wild-type.

introduced. Next, we performed mutagenesis on each of APEX2's seven tyrosine residues (Extended Data Fig. 2j) to identify the location of the tyrosyl radical. EPR analysis of these mutants showed that the tyrosyl radial is hopped or transferred between Y190 and Y224 (Fig. 2i and Extended Data Fig. 2l,n). The tyrosyl radical signal was absent only when both of these two residues were mutated, which led to a complete loss of photoreactivity (Fig. 2j and Extended Data Fig. 2k,m). These results establish that the tyrosyl radical within APEX2, along

with the high-affinity probe BN2, is the key for photoreactivity, and O_2 is necessary (Fig. 2k) for the radical enhancement and photoreactivity (Fig. 2l). This synergistic mechanism enables efficient, H_2O_2-free, light-responsive labeling, advancing the application of the ROProx technology for dynamic protein complex profiling.

The H_2O_2-free photoreactive ROProx system achieves 10-nm spatial resolution

To test the performance of ROProx in labeling protein complex, we adopted the IPP–RSU1 system, a structurally well-resolved protein complex comprising ILK, PINCH, the parvins (PARVA and PARVB) and RSU1 (refs. 31,32). The structure of each protein component was integrated to precisely calculate its distance from the bait protein ILK. By generating a cell line that stably expresses ILK with APEX2–Flag fused to its N terminus, we established a measurable reference framework to evaluate the labeling selectivity of the chemical PL probe at an approximately 10-nm scale (Fig. 3a). Next, we conducted affinity purification–mass spectrometry (AP–MS) analysis to evaluate the labeling efficiency of BN2 and its selectivity for the IPP–RSU1 complex at the proteome level. As expected, treating cells with 500 μM BN2 and 500 μM H_2O_2 led to the selective labeling and identification of the IPP–RSU1 complex components (Extended Data Fig. 3a). Notably, we achieved similar results in the absence of exogenous H_2O_2 (Fig. 3b), whereas the probes BC1 and BC4 did not label all the components (Extended Data Fig. 3b,c). These results demonstrate the successful development of an H_2O_2-free but BN2-dependent and APEX2-dependent PL methodology.

We next investigated the potential of applying ROProx in the AP–MS system. Cells incubated with 500 μM BN2 and exposed to blue light for just 2 minutes unexpectedly led to the selective labeling of the IPP–RSU1 complex (Extended Data Fig. 3d). Notably, reducing the BN2 concentration to 50 μM while maintaining 2 minutes of blue light exposure (Fig. 3c and Supplementary Table 4) produced a cleaner background with minimal non-specific labeling compared to treatment with 500 μM BN2. MS quantification of the IPP–RSU1 complex proteins labeled under these conditions revealed a strong correlation with their spatial proximity to ILK (Fig. 3a). Notably, the distances between these proteins and ILK were less than 10 nm, underscoring the precise and controllable labeling radius enabled by visible light-activated BN2 and APEX2.

We further investigated the mechanism that controls the labeling radius of the ROProx system and contributes to its high specificity. MS analysis of biotinylated peptides from the cells and in vitro experiments demonstrated that BN2 preferentially modified histidine (H) residues (Fig. 3d), with H42 on APEX2 identified as the primary labeling site (Fig. 3e, Extended Data Fig. 3e,f and Supplementary Table 5). Notably, mutation of H42 abolished the photoreactive labeling, establishing H42 as a critical regulatory element—or 'brake'—that defines APEX2 activity and the labeling radius (Fig. 3f and Extended Data Fig. 3g). Interestingly, among all residues, only H42 of APEX2 was found to be modified by BN2, forming a conjugate with the histidine residue via its amino group (Supplementary Figs. 10 and 11)[33]. In addition, BN2 employs a second 'brake' upon polymerization, effectively quenching the excess active BN2 and preventing an extended labeling radius[21]. Together, these dual 'brakes'—H42 self-labeling and BN2 self-quenching—constrain the labeling radius to approximately 10 nm, enabling precise and selective profiling of protein complexes in living systems.

We then compared the performance of this method to those of other H_2O_2-free or photoreactive PL methods, including TurboID, miniSOG and LOV-Turbo. Although applying TurboID effectively led to all five components of the IPP–RSU1 complex being labeled, substantial non-specific labeling was also observed (Extended Data Fig. 3h,i). Compared to LOV-Turbo and miniSOG, BN2 together with APEX2 demonstrated superior photoreactive protein complex labeling (Fig. 3g). Notably, this BN2-dependent and APEX2-dependent PL technique requires only very mild blue light irradiation (34 mW cm^{-2}), which is much less than the light intensity required for LOV-Turbo and miniSOG. Notably, such complete labeling process with mild and short light exposure had subtle effects on cell viability and mitochondrial morphology to cells (Extended Data Fig. 4a–d). Finally, we compared the PL reaction in the nucleus, mitochondria and endoplasmic reticulum, which have different levels of endogenous H_2O_2 (ref. 34), and found that this blue light-dependent PL method has a notable advantage and can compensate for the differences in PL caused by the different levels of endogenous H_2O_2 (Extended Data Fig. 4e).

ROProx-based dynamic protein complex profiling on a timescale of seconds

We further evaluated the ability of ROProx to profile dynamic protein complexes down on a timescale of seconds by stably expressing APEX2–Flag-tagged GRB2 in HeLa cells (Fig. 4a). GRB2 is a key adaptor protein that is recruited into endothelial growth factor receptor (EGFR)-mediated signaling complexes seconds to minutes after EGF stimulation[3,35]. Activation of this signaling pathway is critical for many biological processes and tends to be modulated by H_2O_2 because H_2O_2 functions as a secondary messenger and selectively oxidizes cysteine residues in protein phosphatases and kinases[23]. In this context, the exogenous H_2O_2-free and blue light-dependent PL technology ROProx offers a unique solution. As expected, standard 500 μM H_2O_2-dependent PL effectively captured known EGF stimulation-dependent GRB2-interacting proteins (Extended Data Fig. 5a). However, PL in the absence of H_2O_2 did not capture any of the proteins in the GRB2 interactome (Extended Data Fig. 5b). Notably, as little as 25 μM H_2O_2 was sufficient to label most of the EGF stimulation-dependent GRB2-interacting proteins (Fig. 4b), which is a 20-fold decrease in H_2O_2 concentration compared to standard H_2O_2-dependent PL reactions. Further increasing the H_2O_2 concentration to 100 μM did not result in improved labeling efficiency (Extended Data Fig. 5c). Accordingly, we systematically validated the sufficient PL of interacting proteins EGFR, CBL, SHC1 and STS1 under 25 μM H_2O_2 by affinity purification and western blotting (Extended Data Fig. 5d). Although the exact concentration of H_2O_2 in living cells is unknown, 25 μM is extremely low and should generally address the artificial signaling activation caused by excess H_2O_2.

Next, we tested the performance of ROProx under mild blue light illumination to identify weak and transient protein interactions that occur during signal transduction. Two minutes of blue light irradiation demonstrated remarkable selectivity for capturing GRB2 interactome (Extended Data Fig. 5e). Notably, 30 seconds of light exposure provided superior profiling of transiently interacting proteins (Fig. 4c and Supplementary Table 6). A comparison of the proteins identified upon 25 μM H_2O_2 treatment with 30 seconds of blue light exposure revealed that both conditions led to the consistent labeling of well-characterized GRB2-interacting proteins, such as SHC1, PIK3R2, GAB1 and UBASH3B. However, distinct differences were observed with other well-known GRB2-interacting proteins, including CBL, CBLB, PIK3C2B and PTPN11 (Fig. 4d). Interestingly, 30 seconds of blue light irradiation also labeled several additional proteins that were not captured with 25 μM H_2O_2 treatment. These results highlight the robustness of ROProx for dynamic protein complex profiling and emphasize the need for precise control over labeling conditions in physiologically relevant studies. It should be noted that a recent study revealed protein damage caused by minute-scale blue light exposure, which further demonstrates the advantage of ROProx for photoreactive PL[36].

Because LITag[17] and SOPP3–APEX2 (ref. 14) also demonstrated second-scale labeling capability with distinct mechanisms, we compared them with ROProx for dynamic protein complex profiling. LITag relies on the LOV* domain, which absorbs light and generates singlet oxygen to oxidize nearby protein residues. SOPP3–APEX2 integrates SOPP3, which produces singlet oxygen that is converted by superoxide dismutases (SODs) into H_2O_2 and subsequently activates APEX2

https://doi.org/10.1038/s41589-026-02230-0

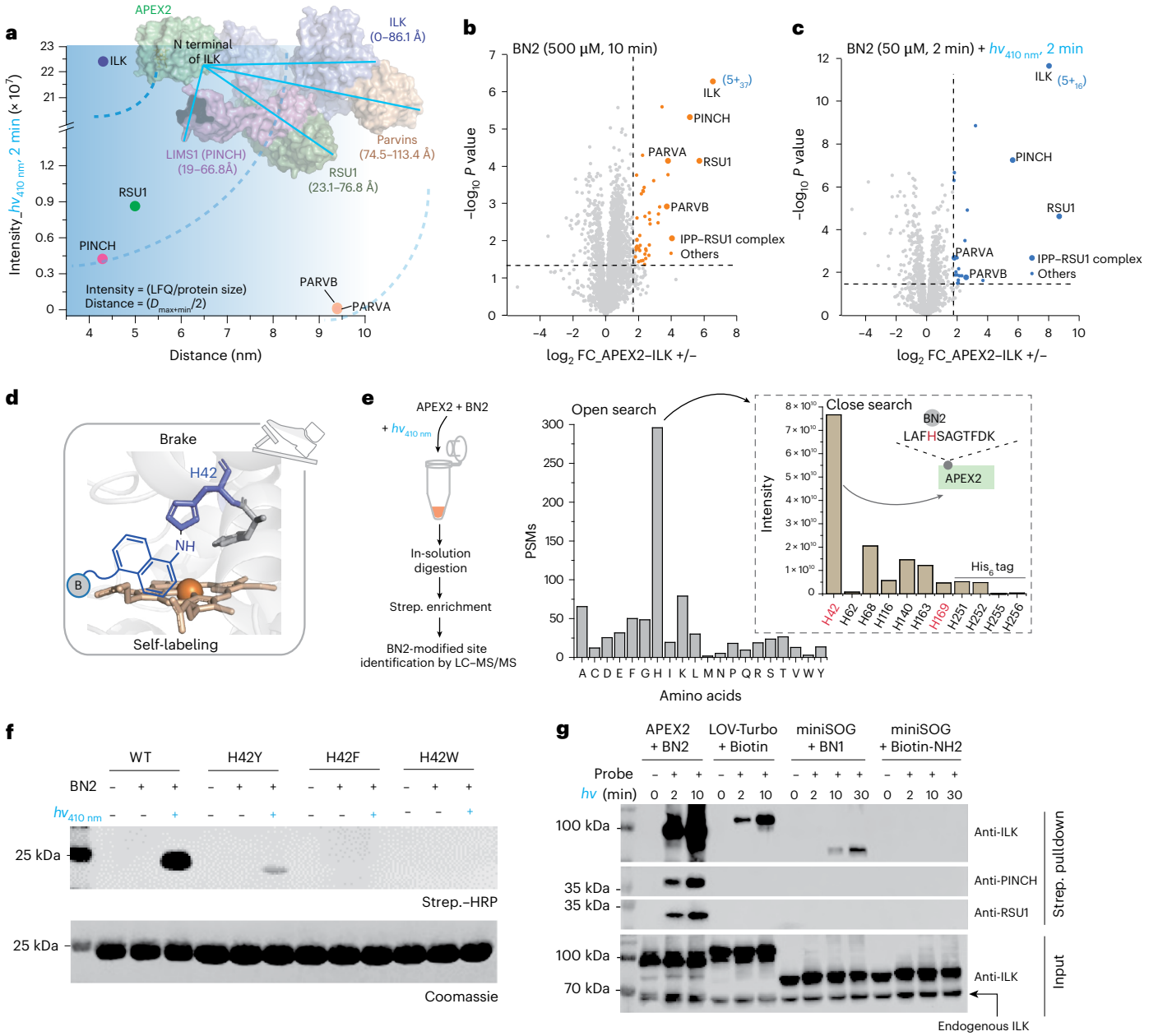

Fig. 3 | The H_2O_2-free photoreactive ROProx system achieves 10-nm spatial resolution. a, Aligned crystal structure of the IPP–RSU1 complex, integrated from ILK–PINCH (PDB: 2KBX), ILK–PARVA (PDB: 3KMU) and RSU1–LIM45C of PINCH (PDB: 7D2U). Distances from the N terminal of ILK were measured in the integrated model, and both distances and MS labeling intensities of the four proteins under blue light activation are shown as a scatter plot. **b**, Volcano plot showing AP–MS results for the IPP–RSU1 complex labeled by BN2 without H_2O_2 (biological replicates $n = 3$, $\log_2FC > 1.8$, $P < 0.05$, two-sided Student's *t*-test, no adjustments). **c**, Volcano plot of AP–MS results for IPP–RSU1 complex labeled with 50 μM BN2 plus blue light exposure for 30 seconds (biological replicates $n = 3$ for APEX2$^-$ group and $n = 5$ for APEX2$^+$ group, $\log_2FC > 1.8$, $P < 0.05$, two-sided Student's *t*-test, no adjustments). **d**, The schematic depicts BN2's self-labeling 'brake' mechanism. **e**, Site preference analysis of BN2 modification on APEX2. Peptide-level analysis of BN2-modified APEX2 reveals site-specific preferences (biological replicates $n = 2$). Bar graphs summarize the relative modification abundance at each site. PSMs, peptide-spectrum matches. **f**, Labeling effects were examined for H42 mutants in which histidine was substituted with tryptophan (W), phenylalanine (F) or tyrosine (Y), residues capable of engaging in hydrogen bonding or π interactions. The experimental group was exposed to 410-nm light for 2 minutes, whereas the control group was kept in the dark (biological replicates $n = 3$). **g**, Comparison of light-dependent labeling by APEX2, photoreactive enzymes LOV-Turbo and miniSOG. Related ILK stable cell lines were treated with 50 μM indicated probes and light with excitation wavelengths of 400–410 nm (APEX2), 465–470 nm (LOV-Turbo) and 460–465 nm (miniSOG) and analyzed by streptavidin pulldown and western blotting (biological replicates $n = 2$). FC, fold change; LC–MS/MS, liquid chromatography–tandem mass spectrometry; LFQ, label-free quantitation; max, maximum; min, minimum; Strep., streptavidin; WT, wild-type.

for PL. Distinctively, ROProx depends on the BN2 probe binding to APEX2 and engages APEX2's intrinsic tyrosyl radical to trigger photoreactive PL. To meet the SOPP3–APEX2's experimental condition and further challenge the ROProx for PL with only 10 seconds of blue light exposure, we compared the PL performance of the three approaches for profiling EGF stimulation-dependent GRB2 interactome (Fig. 4e). Further affinity purification and western blotting validation of CBL and SHC1 interaction both demonstrated that ROProx markedly outperformed LITag and SOPP3–APEX2 under 10-second light exposure (Fig. 4f and Supplementary Table 7).

https://doi.org/10.1038/s41589-026-02230-0

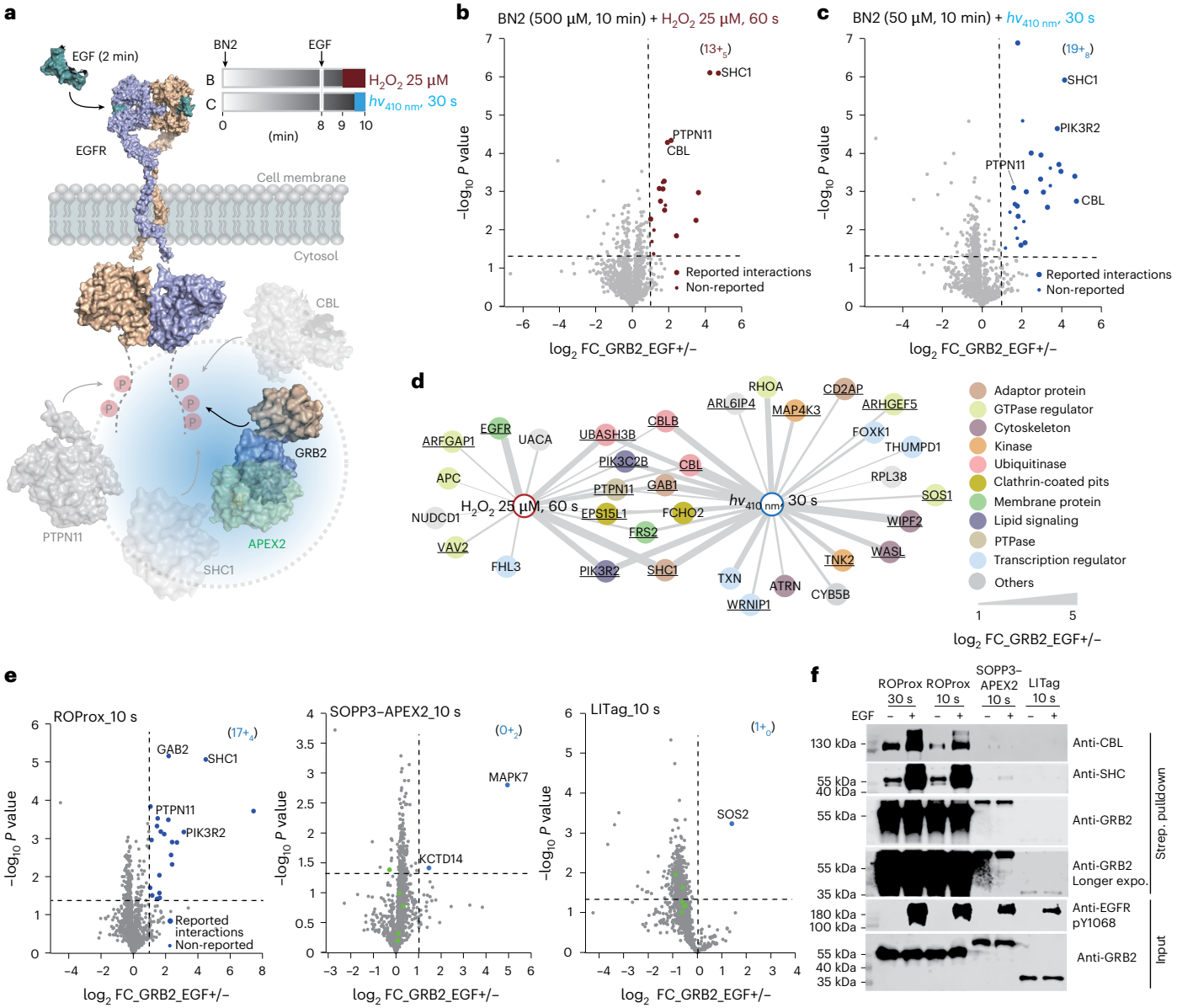

Fig. 4 | Second-scale dynamic protein complex profiling by ROProx. **a**, Schematic illustration for profiling the second-scale dynamic protein complex of GRB2 upon EGF stimulation. The structures of EGF and EGFR are derived from PDB entries 3NJP, 2M20 and 2GS6. The structure of GRB2 is from PDB 1GRI, and the APEX2 structure was solved in this study. The structures of SHC1 (PTB domain), c-Cbl and PTPN11 are based on PDB entries 4XWX, 2Y1M and 3B7O, respectively. **b**,**c**, Volcano plot of AP–MS results for EGF stimulation-dependent GRB2 interactome labeled by incubating 500 μM BN2 for 10 minutes and then 25 μM H_2O_2 for 60 seconds (**b**) and incubating 50 μM BN2 for 10 minutes and blue light irradiation for 30 seconds (**c**). The number of proteins with significant change is highlighted (biological replicates $n = 3$, $\log_2FC > 1$, $P < 0.05$, two-sided Student's *t*-test, no adjustments), with reported interactions[3,35,42,43] marked with larger dots and numbers. **d**, Quantitative comparison and function analysis of the significantly changed proteins identified in **b** and **c**. The reported interacting proteins are underlined. **e**, Comparison of ROProx, SOPP3–APEX2 and LITag in profiling the EGF stimulation-dependent interactome of GRB2. The dots labeled in green represent interacting proteins identified by ROProx but not significant in SOPP3–APEX2 or LITag experiments (biological replicates $n = 3$, $\log_2FC > 1$, $P < 0.05$, two-sided Student's *t*-test, no adjustments). **f**, Streptavidin pulldown–western blotting validation of indicated proteins by the three PL methods (biological replicates $n = 2$). FC, fold change; Strep., streptavidin; Expo., exposure.

Dynamic GRB2 interactome mapping in living mice using ROProx

The limited penetration depth of light presents a considerable challenge for photoreactive PL in vivo. However, the low H_2O_2 dependency of ROProx technology mitigates this limitation by operating effectively at endogenous H_2O_2 level. To evaluate the in vivo PL performance of ROProx, we generated transgenic mice expressing APEX2–Flag-tagged Grb2, with successful integration confirmed by genotyping polymerase chain reaction (PCR) using tail-tip genomic DNA (Fig. 5a,b). We first measured endogenous H_2O_2 levels using the HKPerox-2 probe[37], revealing dynamic H_2O_2 distribution across different organs (Fig. 5c). Subsequently, the BN2 probe was administered via intravenous injection, and, after a 5-minute circulation period, efficient labeling of Grb2 was observed in multiple major organs (Fig. 5d). The labeling intensity varied among tissues and correlated well with the endogenous H_2O_2 levels. Notably, the spleen exhibited the lowest labeling efficiency, consistent with its low endogenous H_2O_2 level. Although light-inducible PL is not optimal for in vivo application due to limited light penetration, we tested its feasibility for PL in spleen as a complementary approach where endogenous H_2O_2 is too low. Notably, a 5-minute exposure to blue

https://doi.org/10.1038/s41589-026-02230-0

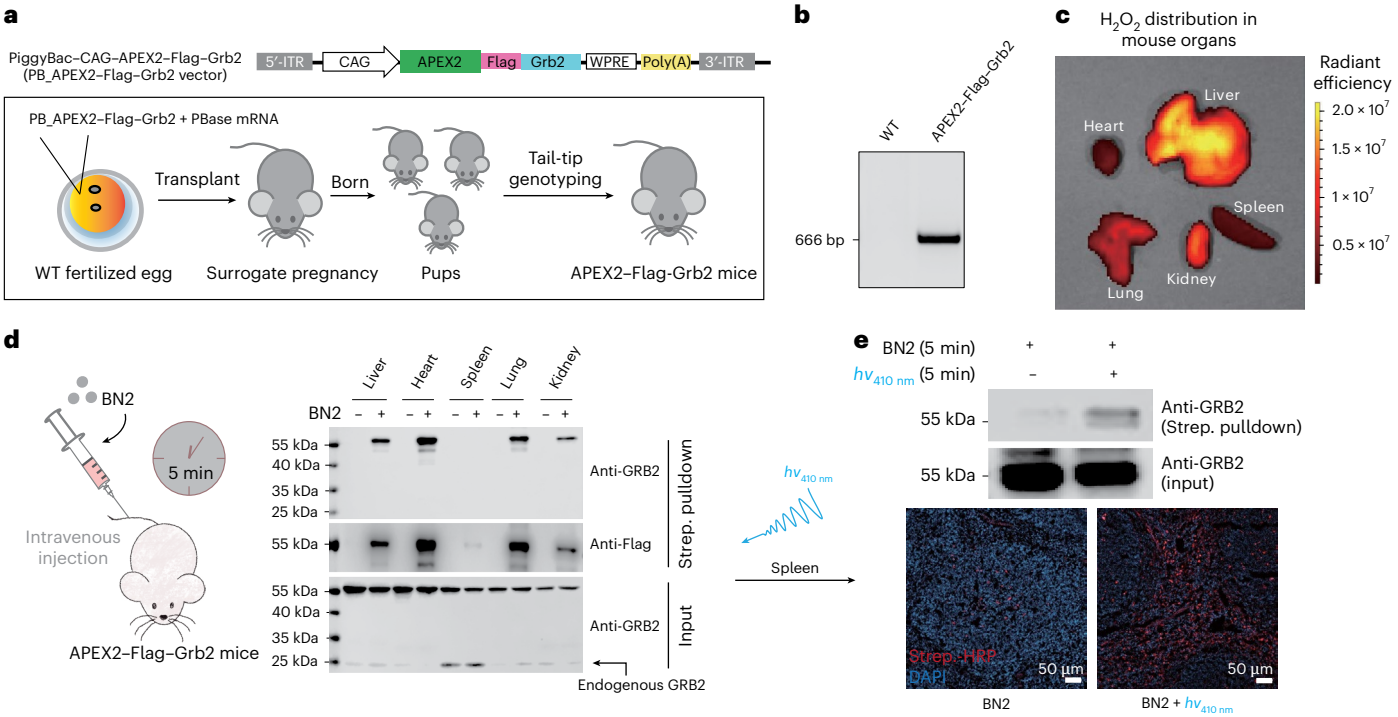

Fig. 5 | ROProx application in transgenic mice expressing APEX2–Flag-tagged Grb2. a, Generation of transgenic mice ubiquitously overexpressing APEX2–Flag-tagged Grb2. The PiggyBac system plasmid encoding APEX2–Flag-tagged Grb2, along with PBase mRNA, was microinjected into fertilized eggs, which were then implanted into the uterus of a surrogate mouse. After birth, pups were screened for APEX2–Flag-tagged Grb2 expression by genotyping PCR using tail-tip genomic DNA. For detailed methods, see the Supplementary Methods. **b**, TAIL-PCR screening of mice for APEX2–Flag–Grb2 fusion expression. Bands represent the length corresponding to APEX2 and partial Grb2 nucleotide sequences ($n = 3$ mice for wild-type and APEX2–Flag–Grb2 mice, respectively). **c**, Physiological distribution of endogenous H_2O_2 in the liver, heart, spleen, lung and kidney, detected using the HKPerox 2 probe (biological replicates $n = 3$ mice). **d**, The efficiency of BN2 in labeling the bait protein Grb2 in different organs was assessed via intravenous injection and streptavidin pulldown (biological replicates $n = 3$). **e**, Assessment of BN2 labeling efficiency in the spleen before and after blue light irradiation, analyzed through streptavidin pulldown–western blotting (biological replicates $n = 3$) and streptavidin–Cy3 immunofluorescence (biological replicates $n = 3$). bp, base pairs; ITR, inverted terminal repeat; Strep., streptavidin; WT, wild-type.

light assisted by surgical exposure significantly enhanced labeling in the spleen (Fig. 5e), which is approximately 2 mm thick, corresponding to the penetration depth of blue light, demonstrating the capacity of ROProx to boost PL efficiency in vivo.

To further evaluate its in vivo PL performance by taking advantage of its second-mode PL, which is sensitive to extremely low H_2O_2, we applied ROProx to explore pTyr-mediated dynamic interactome of Grb2 in liver upon 2 minutes of EGF stimulation or upon liver partial hepatectomy (2/3 PHx) by hepatic portal vein injection of BN2 for 5 minutes (Fig. 6a). Global pTyr site profiling was also performed to systematically recapitulate the in vivo pTyr machinery. To balance the physiological state of the living mice and efficient labeling, a timecourse experiment was performed, and it was determined that optimal labeling occurred 5 minutes after BN2 injection (Fig. 6b). This approach enabled the identification of Grb2 and its well-characterized dynamic interactome, including Egfr and Shc1 (Extended Data Fig. 6a and Supplementary Table 8). Approximately 400 phosphorylation sites in each sample were identified and demonstrated strong consistency across replicates (Extended Data Fig. 6b–d). Two-dimensional analysis of the Grb2 interactome and the identified pTyr sites revealed the critical roles of Egfr, Shc1 and other signaling proteins in mediating pTyr-dependent signal transduction during EGF stimulation in vivo (Fig. 6c,d). Among them, Slc25a4 was identified as a new interacting protein of Grb2, with pTyr occurring at Y195 (Fig. 6e). Slc25a4 is an ADP/ATP transporter and plays a pivotal role in energy homeostasis by facilitating nucleotide exchange across the inner mitochondrial membrane[38]. This novel discovery, validated through co-immunoprecipitation experiments in HEK293T cells (Fig. 6f), reveals the previously unknown roles of Grb2 in mitochondrial dynamics, expanding our understanding of its functional repertoire in cellular signaling and metabolism.

The liver is one of the very few organs in mammals capable of regeneration after removal or injury. Many studies have reported that liver regeneration involves the activation of pTyr machinery[39]. To uncover these signaling events that occur during liver regeneration, we performed ROProx-based Grb2 interactome, global pTyr site and total proteome profiling 2 days after 70% PHx in mice (Fig. 6a and Extended Data Fig. 6e,g). The evident cell proliferation observed via Ki67 staining confirmed ongoing liver regeneration in these mice (Fig. 6g). As expected, ROProx-based protein complex profiling revealed increased association of proteins such as Pcna[40] and Mcm6 (ref. 41), which are known to upregulate during liver cell proliferation (Fig. 6h and Extended Data Fig. 6e). Interestingly, we discovered that the change of Cdk1 within the protein complex was far greater than that in the total proteome (Extended Data Fig. 6g). Moreover, global pTyr profiling revealed that Cdk1 Y15 phosphorylation and EGFR signaling components were significantly upregulated upon PHx (Fig. 6h and Extended Data Fig. 6f). The association of Cdk1 with Grb2 was further validated by streptavidin pulldown–western blotting and Flag immunoprecipitation–western blotting in tissue lysates and by immunoprecipitation–western blotting in cell lysates (Fig. 6i and Extended Data Fig. 6h). In addition, phosphorylation of CDK1 at its Y15 site after 2/3 PHx was also confirmed (Fig. 6i). These findings suggest the signaling role of Cdk1 and Grb2 during liver regeneration and demonstrate the high efficiency, selectivity and biocompatibility of ROProx for labeling dynamic protein complexes in living animals on the timescale of minutes.

https://doi.org/10.1038/s41589-026-02230-0

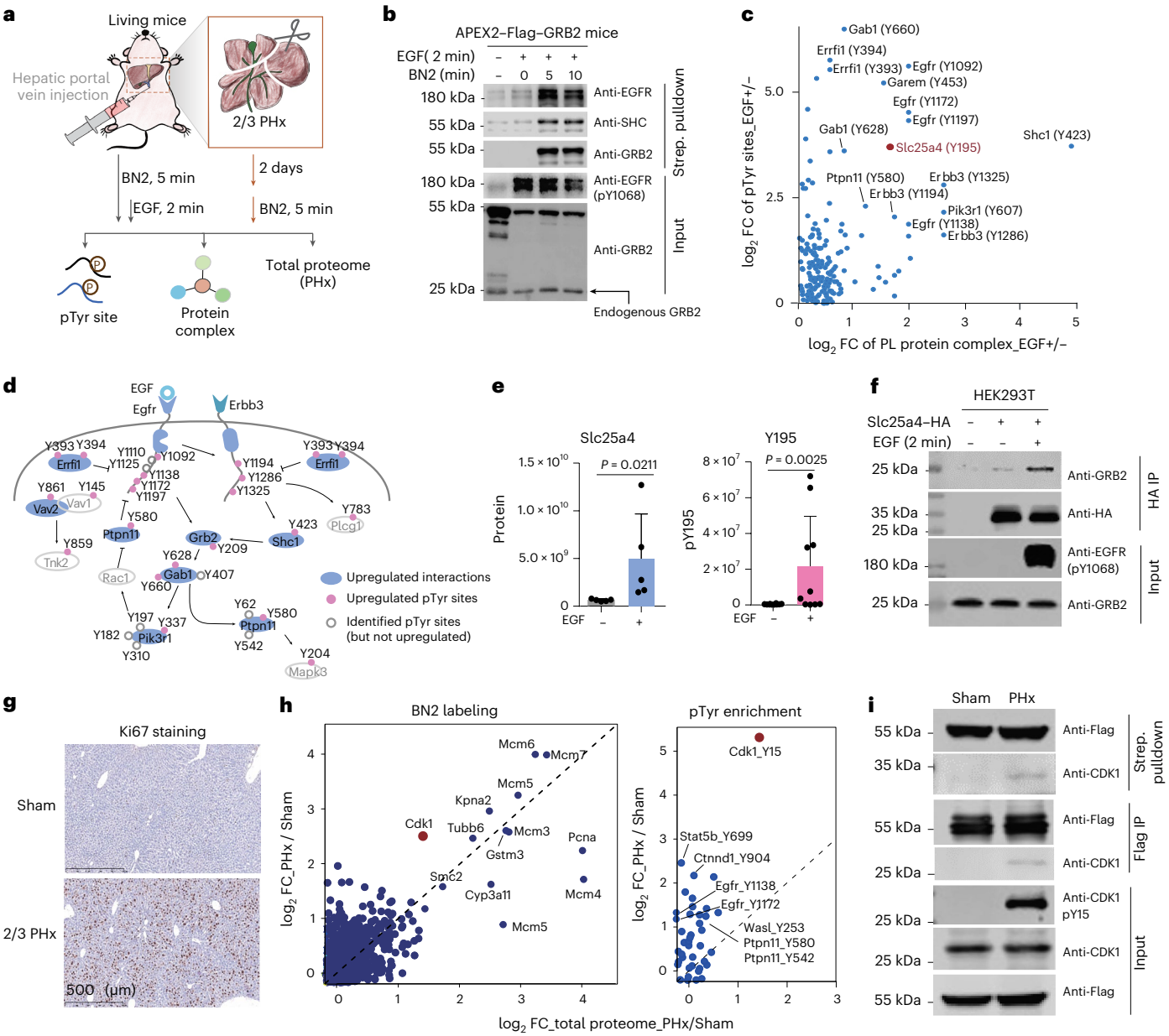

Fig. 6 | Dynamic Grb2 interactome mapping in living mice by ROProx. **a**, Schematic representation of BN2-mediated PL in mapping the pTyr sites and dynamic Grb2 interactome in vivo upon EGF stimulation or in the 2/3 PHx liver regeneration model. The total proteome was also analyzed in the liver regeneration system to account for expression changes over the 2-day progression. BN2 and/or EGF was injected into liver through the hepatic portal vein when the mouse was anesthetized. **b**, Investigation of the optimal injection time for BN2, as assessed by streptavidin pulldown–western blotting GRB2-associated proteins EGFR and SHC1 (biological replicates $n = 3$). **c**, Two-dimensional quantitative analysis of Grb2-interacting proteins by synergistic comparison of the fold changes of both proteins and associated pTyr sites ($n = 5$ mice for EGF + BN2 and BN2 groups, respectively). **d**, Identified key functional proteins and their associated pTyr sites in the EGFR signaling pathway. **e**, LFQ intensities of Slc25a4 and intensities of its pY195 identified in the in vivo ROProx labeling ($n = 5$ mice for EGF + BN2 and BN2 groups, respectively). Regarding the pTyr sites data, duplicate samples were collected from each mouse, providing 10 data points in each group. Data are presented as mean values ± s.e.m. **f**, Validation of Slc25a4 interaction with Grb2 in an EGF stimulation-dependent manner in HEK293T cells using HA tag immunoprecipitation–western blotting (biological replicates $n = 3$). **g**, Ki67 staining to assess liver regeneration in mice after the removal of two-thirds of the liver after 2 days ($n = 3$ mice for 2/3 PHx and sham groups, respectively). **h**, Quantitative analysis of Grb2-interacting proteins by integrating fold change comparisons of protein levels and associated pTyr site modifications ($n = 7$ mice for PHx and sham groups, respectively). The proteins and pTyr sites with significant change are labeled. **i**, Validation of the interaction between Grb2 and Cdk1 using streptavidin pulldown and Flag immunoprecipitation in liver tissue lysates followed by western blotting analysis (biological replicates $n = 3$). IP, immunoprecipitation; Strep., streptavidin.

Discussion

PL together with MS-based proteomics has become increasingly popular for exploring functional proteome with spatial proximity in living systems. As compared with subproteome and stable protein complex profiling, dynamic protein complex profiling, especially at a timescale of minutes to seconds, has been the most challenging perspective. Although ascorbate peroxidase APEX2 is well suitable for this application, benefiting with its fast and robust kinetics, its H_2O_2 reliance is the well-recognized limitation for dynamic protein complex profiling in living and H_2O_2-sensitive systems. Many pioneer PL

technology developments have been achieved recently for reducing the labeling radius and labeling time and controlling the labeling reaction by photoreactivity. These efforts largely fall into two categories: first, introduction of new PL enzymes, best represented by peroxidase, biotin ligase families, singlet oxygen generation families (SOPP3, miniSOG, LOV and LITag) or direct evolution of these PL enzymes; second, development of small molecular photoreactive catalysts, best represented by μ-Map and MultiMap. However, H_2O_2-free proximity proteomic profiling of dynamic protein complexes at second-scale time resolution and less than 10-nm labeling radius scale in living systems is still challenging.

In the present study, we adopted a different strategy for chemically evolving substrate probes of APEX2 that have no reliance on exogenous H_2O_2 and are photoreactive. We developed the ROProx system based on BN2 probe and APEX2, which well meet these two criteria. The tyrosyl radical, as well as the high binding affinity of BN2 to APEX2, can be activated by blue light, enabling the precise and efficient profiling of dynamic protein complexes in living cells. Additionally, the unique dual 'brake' mechanism precisely controls labeling radius of 10 nm in living systems while achieving resolution on a timescale of minutes to seconds. It is worth noting that prolonged minute-scale blue light exposure in living cells can induce protein damage and attenuate phosphorylation-dependent signaling, as systematically demonstrated by Toh et al.[36]. Accordantly, second-scale labeling by ROProx largely avoids this commonly encountered issue. In addition, BN2 has two additional characteristics: (1) its high susceptibility to oxidation and (2) its capacity for self-polymerization. These properties collectively enable its optimal performance in peroxidase-mediated PL. Alternatively, BN2 is also sensitive to extremely low levels of H_2O_2 and even endogenous H_2O_2 for robustly capturing dynamic protein complexes in living cells and living mice. Mechanistically, the two modes operate in a complementary manner: light-responsive ROProx preferentially labels histidine residues (Fig. 3e), whereas H_2O_2-mediated labeling favors tyrosine residues[21]. Collectively, the chemical evolution of classic H_2O_2-dependent ascorbate peroxidase revealed unexpected molecular mechanisms and dual-modal PL, which open new avenues for exploring novel PL functionality toward challenging but critical application in dynamic protein machinery studies.

Online content

Any methods, additional references, Nature Portfolio reporting summaries, source data, extended data, supplementary information, acknowledgements, peer review information; details of author contributions and competing interests; and statements of data and code availability are available at https://doi.org/10.1038/s41589-026-02230-0.

References

1. Alberts, B. The cell as a collection of protein machines: preparing the next generation of molecular biologists. *Cell* **92**, 291–294 (1998).
2. Olsen, J. V. et al. Global, in vivo, and site-specific phosphorylation dynamics in signaling networks. *Cell* **127**, 635–648 (2006).
3. Bisson, N. et al. Selected reaction monitoring mass spectrometry reveals the dynamics of signaling through the GRB2 adaptor. *Nat. Biotechnol.* **29**, 653–658 (2011).
4. Zheng, Y. et al. Temporal regulation of EGF signalling networks by the scaffold protein Shc1. *Nature* **499**, 166–171 (2013).
5. Scott, J. D. & Pawson, T. Cell signaling in space and time: where proteins come together and when they're apart. *Science* **326**, 1220–1224 (2009).
6. Attwood, M. M., Fabbro, D., Sokolov, A. V., Knapp, S. & Schioth, H. B. Trends in kinase drug discovery: targets, indications and inhibitor design. *Nat. Rev. Drug Discov.* **20**, 839–861 (2021).
7. Sharma, P. et al. Immune checkpoint therapy-current perspectives and future directions. *Cell* **186**, 1652–1669 (2023).
8. Roux, K. J., Kim, D. I., Raida, M. & Burke, B. A promiscuous biotin ligase fusion protein identifies proximal and interacting proteins in mammalian cells. *J. Cell Biol.* **196**, 801–810 (2012).
9. Go, C. D. et al. A proximity-dependent biotinylation map of a human cell. *Nature* **595**, 120–124 (2021).
10. Uezu, A. et al. Identification of an elaborate complex mediating postsynaptic inhibition. *Science* **353**, 1123–1129 (2016).
11. Droujinine, I. A. et al. Proteomics of protein trafficking by in vivo tissue-specific labeling. *Nat. Commun.* **12**, 2382 (2021).
12. Kim, K. E. et al. Dynamic tracking and identification of tissue-specific secretory proteins in the circulation of live mice. *Nat. Commun.* **12**, 5204 (2021).
13. Wei, W. et al. Cell type-selective secretome profiling in vivo. *Nat. Chem. Biol.* **17**, 326–334 (2021).
14. Qu, D. et al. Photoactivated SOPP3 enables APEX2-mediated proximity labeling with high spatio-temporal resolution in live cells. *Cell Res.* **35**, 149–152 (2025).
15. Wang, P. et al. Mapping spatial transcriptome with light-activated proximity-dependent RNA labeling. *Nat. Chem. Biol.* **15**, 1110–1119 (2019).
16. Lee, S. Y. et al. Engineered allostery in light-regulated LOV-Turbo enables precise spatiotemporal control of proximity labeling in living cells. *Nat. Methods* **20**, 908–917 (2023).
17. Hananya, N., Ye, X., Koren, S. & Muir, T. W. A genetically encoded photoproximity labeling approach for mapping protein territories. *Proc. Natl Acad. Sci. USA* **120**, e2219339120 (2023).
18. Lam, S. S. et al. Directed evolution of APEX2 for electron microscopy and proximity labeling. *Nat. Methods* **12**, 51–54 (2015).
19. Paek, J. et al. Multidimensional tracking of GPCR signaling via peroxidase-catalyzed proximity labeling. *Cell* **169**, 338–349 (2017).
20. Lobingier, B. T. et al. An approach to spatiotemporally resolve protein interaction networks in living cells. *Cell* **169**, 350–360 (2017).
21. Ke, M. et al. Spatiotemporal profiling of cytosolic signaling complexes in living cells by selective proximity proteomics. *Nat. Commun.* **12**, 71 (2021).
22. Liu, G. et al. Mechanism of adrenergic $Ca_V1.2$ stimulation revealed by proximity proteomics. *Nature* **577**, 695–700 (2020).
23. Rhee, S. G. Cell signaling. H_2O_2, a necessary evil for cell signaling. *Science* **312**, 1882–1883 (2006).
24. Rhee, H. W. et al. Proteomic mapping of mitochondria in living cells via spatially restricted enzymatic tagging. *Science* **339**, 1328–1331 (2013).
25. Buksh, B. F. et al. muMap-Red: proximity labeling by red light photocatalysis. *J. Am. Chem. Soc.* **144**, 6154–6162 (2022).
26. Lin, Z. et al. Multiscale photocatalytic proximity labeling reveals cell surface neighbors on and between cells. *Science* **385**, eadl5763 (2024).
27. Jones, D. K., Dalton, D. A., Rosell, F. I. & Raven, E. L. Class I heme peroxidases: characterization of soybean ascorbate peroxidase. *Arch. Biochem. Biophys.* **360**, 173–178 (1998).
28. Patterson, W. R. & Poulos, T. L. Crystal structure of recombinant pea cytosolic ascorbate peroxidase. *Biochemistry* **34**, 4331–4341 (1995).
29. Patterson, W. R., Poulos, T. L. & Goodin, D. B. Identification of a porphyrin pi cation radical in ascorbate peroxidase compound I. *Biochemistry* **34**, 4342–4345 (1995).
30. Lucic, M. et al. New insights into controlling radical migration pathways in heme enzymes gained from the study of a dye-decolorising peroxidase. *Chem. Sci.* **14**, 12518–12534 (2023).
31. Sepulveda, J. L. & Wu, C. The parvins. *Cell. Mol. Life Sci.* **63**, 25–35 (2006).

32. Yang, H. et al. Complex structures of Rsu1 and PINCH1 reveal a regulatory mechanism of the ILK/PINCH/Parvin complex for F-actin dynamics. *eLife* **10**, e64395 (2021).
33. Zhai, Y. et al. Global profiling of functional histidines in live cells using small-molecule photosensitizer and chemical probe relay labelling. *Nat. Chem.* **16**, 1546–1557 (2024).
34. Lei, S. et al. Sensitive subcellular scale and real-time detection of hydrogen peroxide by a W-doped Pt microelectrode. *Chem. Commun. (Camb)* **60**, 7630–7633 (2024).
35. Kong, Q. et al. Dynamic phosphotyrosine-dependent signaling profiling in living cells by two-dimensional proximity proteomics. *J. Proteome Res.* **21**, 2727–2735 (2022).
36. Toh, K. et al. Chemoproteomic identification of blue-light-damaged proteins. *J. Am. Chem. Soc.* **144**, 20171–20176 (2022).
37. Ye, S., Hu, J. J. & Yang, D. Tandem payne/dakin reaction: a new strategy for hydrogen peroxide detection and molecular imaging. *Angew. Chem. Int. Ed. Engl.* **57**, 10173–10177 (2018).
38. Kunji, E. R. S., King, M. S., Ruprecht, J. J. & Thangaratnarajah, C. The SLC25 carrier family: important transport proteins in mitochondrial physiology and pathology. *Physiology (Bethesda)* **35**, 302–327 (2020).
39. Michalopoulos, G. K. & Khan, Z. Liver regeneration, growth factors, and amphiregulin. *Gastroenterology* **128**, 503–506 (2005).
40. Assy, N. et al. Use of proliferating cell nuclear antigen as a marker of liver regeneration after partial hepatectomy in rats. *J. Lab. Clin. Med.* **131**, 251–256 (1998).
41. Liu, M. et al. MCM6 promotes metastasis of hepatocellular carcinoma via MEK/ERK pathway and serves as a novel serum biomarker for early recurrence. *J. Exp. Clin. Cancer Res.* **37**, 10 (2018).
42. Caron, E. et al. Precise temporal profiling of signaling complexes in primary cells using SWATH mass spectrometry. *Cell Rep.* **18**, 3219–3226 (2017).
43. Ke, M. et al. Integrated and quantitative proteomic approach for charting temporal and endogenous protein complexes. *Anal. Chem.* **90**, 12574–12583 (2018).

Methods

LED-based blue light exposure

For ROProx, blue light was provided by an LED lamp with a wavelength of 410 nm, positioned 9 cm above the cells or tubes, delivering an intensity of 34 mW cm^{-2}. The light exposure duration was limited to a maximum of 10 minutes to ensure that the temperature remained below 37 °C. For LOV-Turbo, the light wavelength was 465–470 nm with an intensity of 52 mW cm^{-2}, and, for miniSOG, the light wavelength was 460–465 nm with an intensity of 58 mW cm^{-2}.

For SOPP3–APEX2 and LITag in profiling the EGF-stimulated dynamic interactome of GRB2, GRB2 was N-terminally fused with Flag–APEX2–SOPP3 or Flag–LOV* and stably expressed in HeLa cells via lentivirus transduction. SOPP3–APEX and LITag labeling were carried out using BP1 (500 µM) and BN1 (250 µM), respectively. Probes were incubated with cells in the dark for 60 minutes (BP1) or 30 minutes (BN1); EGF was added at the final 2 minutes, and blue light was applied for the last 10 seconds. Light intensities are 50 mW cm^{-2} for SOPP3–APEX2 and 450 mW cm^{-2} for LITag.

Cell culture and PL in living cells

Cell lines were established as previously described[21]. The HEK293T and HeLa cell lines used in this study were sourced from the National Collection of Authenticated Cell Cultures (NCACC) (HEK293T: CSTR 19375.09.3101HUMGNHu44; HeLa: CSTR 19375.09.3101HUMTCHu187). From these, we generated stable cell lines expressing specific tagged proteins. All the cell lines from NCACC were authenticated by the NCACC. Additionally, the HEK293T APEX2–OMM cell line was a gift from P. Zou's laboratory (Peking University), and the HT1080 cell line was kindly provided by C. Wu's laboratory (Southern University of Science and Technology (SUSTech)). HT1080, HeLa and HEK293T stable cell lines were cultured in MEM (HT1080) or DMEM (HeLa, HEK293T) supplemented with 10% FBS (v/v), 1% penicillin–streptomycin (v/v) and puromycin at concentrations of 1 µg ml^{-1} (HT1080) or 0.6 µg ml^{-1} (HeLa). For APEX2–Flag expression, doxycycline (0.8 µg ml^{-1}) was added to the medium for approximately 20 hours unless specified otherwise.

For screening probes that can label protein complexes without external H_2O_2, prewarmed probes (at 500 µM) were incubated with APEX2–Flag-expressing HT1080 cells at 37 °C for 10 minutes. After washing six times with DPBS, cells were lysed in RIPA buffer containing 50 mM Tris (pH 8.0), 150 mM NaCl, 0.1% SDS (w/v), 0.5% sodium deoxycholate (w/v), 1% Triton X-100 (v/v) and 1 mM EDTA. For positive controls, BP1-treated cells were supplemented with 500 µM H_2O_2. To evaluate ROProx performance in labeling the IPP–RSU1 protein complex, doxycycline was added or omitted to induce or suppress APEX2/Turbo expression, thereby generating $APEX2^{+}Turbo^{+}$ and $APEX2^{-}Turbo^{-}$ groups.

In experiments assessing dynamic interactions, HeLa cells expressing APEX2–Flag–GRB2 were treated with EGF (100 ng ml^{-1}) for 2 minutes before the end of BN2 incubation. H_2O_2 was added at the indicated concentrations 60 seconds before the experiment's conclusion. Blue LED light was turned on 2 minutes, 30 seconds or 10 seconds before the end of the experiment. During processing, the blue light triggered labeling; the room light was off or on as specifically annotated. Streptavidin pulldown was performed as previously described[21]. In brief, after completion of the labeling procedure and cell lysis, samples were sonicated and centrifuged at 17,000*g* and 4 °C for 10 minutes to clarify the lysates. For pulldown experiments, the clarified lysates were incubated with 60 µl of streptavidin Sepharose beads (GE Healthcare, 17-5113-01) overnight at 4 °C. After pulldown, the beads were washed sequentially with strong RIPA buffer (twice), 2 M urea in 10 mM Tris (pH 8.0; twice), 1 M KCl in 10 mM Tris (pH 8.0; twice) and, finally, 50 mM ammonium bicarbonate (ABC) (three times). After washing, the beads were either resuspended in 1× protein loading buffer for subsequent western blotting analysis or subjected to on-bead trypsin digestion, as described in the Supplementary Methods.

Animal welfare and ethics

C57BL/6J mice (6–8 weeks old, approximately 18 g) were used for animal experiments. Mice were housed in specific pathogen-free animal rooms (2–6 mice per cage) with 12-hour light/dark cycles and access to food and water. All animal procedures were approved and conducted in accordance with the guidelines of the Laboratory Animal Center (approval no. SUSTech-JY202201025-202402A1) at SUSTech.

PHx

Six-to-eight-week-old male APEX2–Flag–Grb2 mice were subjected to 70% PHx. In brief, the mice were anesthetized with isoflurane, and a vertical incision was made just below the sternum to adequately expose the liver. The left lateral lobe and the median lobe of the liver were carefully ligated and removed with 4–0 silk suture while the gall bladder was left intact. For the sham-operated controls, the mice were also anesthetized, and the abdominal cavity was entered via incision but without tying off or removing any liver lobes. Once the surgery was done, the abdominal muscles were meticulously stitched up with 6–0 silk thread, and the skin was closed with wound clips. Two days after surgery, all mice were anesthetized, and then BN2 labeling was performed. Subsequently, the mice were euthanized, and the liver tissues were collected and divided into two parts; one part was flash frozen in liquid nitrogen for later proteomic experiments, and the other part was fixed in 4% paraformaldehyde (w/v) for histological analysis.

PL in vivo

To perform PL in living mice across multiple organs, anesthetized mice were injected with BN2 (32 mg kg^{-1}) via the caudal vein. Five minutes after BN2 administration, the mice were euthanized, and the liver, heart, spleen, lung and kidney were harvested and stored in liquid nitrogen. For enhanced labeling efficiency in the spleen, blue light exposure was applied. Anesthetized mice underwent a small skin incision to expose the spleen. BN2 (32 mg kg^{-1}) was administered via the caudal vein, and a blue light source was positioned 9 cm above the exposed spleen, delivering an intensity of 34 mW cm^{-2}. Blue light was applied for a total of 5 minutes, with 2.5 minutes of exposure on each side of the spleen to ensure adequate light penetration. In the control group, anesthetized mice received BN2 injections but were kept in darkness for 5 minutes before tissue harvesting.

For PL in the liver, transgenic mice (approximately 18 g) were anesthetized with 2.5% avertin (12 µl g^{-1}, v/v) via intraperitoneal injection. Once fully anesthetized, the mice were positioned supine on an operating table with their limbs secured. Using surgical scissors and forceps, an incision was made in the lower abdomen to expose the liver and hepatic portal vein. A 24-gauge retention needle with a heparin cap was inserted into the hepatic portal vein, and BN2 (32 mg kg^{-1}, 5 minutes) or EGF (100 µg kg^{-1}, 2 minutes) was injected in a saline solution. BN2 was injected first, followed by an EGF + BN2 mixture 2 minutes before the end of labeling. Afterwards, the mice were euthanized, and the organs were collected and immediately frozen in liquid nitrogen.

Animal sample processing and streptavidin pulldown methodology

After performing in vivo PL and harvesting the organs, the liver was ground into a fine powder using a mortar with liquid nitrogen, replenished frequently. The powdered liver was transferred to a tube and stored in liquid nitrogen until streptavidin pulldown. For the heart, spleen, lung and kidney, tissues were homogenized directly. Each tissue was placed in a 2-ml grinding tube containing 8–10 ceramic particles (Φ 2–3 mm), followed by the addition of 1 ml of ice-cold RIPA buffer supplemented with 1 mM phenylmethylsulfonyl fluoride (PMSF). The tubes were then processed using a tissue homogenizer (MO BIO, PowerLyzer). The homogenizer was set to a vibration speed of 2,500 r.p.m., with each cycle lasting 3 minutes and a 5-second pause

after every 10 seconds of vibration. Four cycles were performed to ensure thorough homogenization.

After homogenization, the lysates were transferred to 2-ml tubes, and an additional 1 ml of ice-cold RIPA buffer was added. The samples were then sonicated for three rounds, each lasting 5 seconds per round. After sonication, the samples were centrifuged at 16,612*g* at 4 °C for 20 minutes, and the supernatants were harvested. Protein concentration was measured using the Pierce 660-nm protein assay (Thermo Fisher Scientific, 22660), and 6 mg of protein was used for streptavidin pulldown. To eliminate excess BN2 probe, the proteins were first purified using a PD-10 desalting column (GE Healthcare, 17085101) according to the manufacturer's protocol. Next, 60 µl of streptavidin Sepharose beads (GE Healthcare, 17-5113-01) was added to the protein solution and incubated overnight at 4 °C on a rotator set to 25 r.p.m.

For pTyr peptide enrichment, 3 mg of liver lysates was used. The protocol for pTyr peptide enrichment was the same as that described in our previous work[21]. In brief, EGF-responsive pTyr signaling was sequentially enriched by the engineered 'superbinder' domain and Ti^{4+}-IMAC microbeads.

Crystallization and structure determination

Crystallization was conducted using vapor diffusion at 16 °C with a reservoir containing 21% PEG 2000 (w/v) MME, 0.1 M Tris-HCl (pH 8.5) and 10 mM $NiCl_2$. Diffraction-quality crystals were cryoprotected in 25% glycerol (v/v) and flash cooled in liquid nitrogen. X-ray diffraction data were collected at the 19U1 beamline at the Shanghai Synchrotron Radiation Facility, processed using HKL2000 and solved via molecular replacement with Phenix, using APX2 (PDB: 5L86) as the search model. Final structure refinement was performed in Phenix with model building in Coot; the detailed statistics are shown in Supplementary Table 1. Details have been deposited in the PDB with ID 9KOE.

BLI for binding affinity

BN2 or BP1 (1 µM) was first stabilized on eight super-sensitive avidin sensors (Sartorius, 18-0011) according to the manufacturer's instructions. HRP, APEX2, APEX2's H169A mutant or APX was diluted to various concentrations (in µM): 0, 0.46, 37 and 111. A 300-µl aliquot of each dilution was placed in one column (eight wells) of a 96-well black plate. The dilution buffer consisted of 50 mM Tris (pH 7.4) and 150 mM NaCl, and the solution was filtered through 0.22-µm filters before use. The dilution buffer was used before and after probe stabilization and protein association. The association of proteins to the stabilized BN2 or BP1 was monitored by the Octet Red 96 system at SUSTech. The K_d values between the proteins and probes were calculated using Octet BLI analysis software.

EPR spectroscopy

The EPR samples of APEX2/APX and the mutants were prepared at a concentration of 20 µg $µl^{-1}$, equivalent to approximately 714 µM. HRP was purchased from Sigma-Aldrich (P6782) and was prepared at a concentration of 714 µM for EPR analysis. The protein samples (200 µl) were transferred into X-band EPR tubes (O.D. 4 mm and I.D. 3 mm), flash frozen and stored in liquid nitrogen for EPR analysis. For the sample of APEX2/APX + BN2, APEX2/APX was mixed with 1 equivalent of BN2 and allowed to react for 5–10 seconds before freezing. For the sample of APEX2/APX + BN2 + *hν*, the APEX2/APX + BN2 mixture was thawed at room temperature, exposed to 410-nm blue light for 5 minutes and then refrozen in liquid nitrogen. Anaerobic samples were performed in a N_2 gas-filled glovebox. PBS was stored in the glovebox for at least 2 days before use. At least three rounds of buffer exchange were performed for APEX2 protein by using a 10-kDa (Millipore) ultrafiltration tube before making the EPR samples.

X-band (9.35 GHz) continuous-wave EPR spectra were recorded on a Bruker EleXsys E500 spectrometer equipped with a super-high Q resonator (ER4122SHQE) in the Department of Chemistry at SUSTech. Cryogenic temperatures were obtained and controlled by using an ESR900 liquid helium cryostat in conjunction with a temperature controller (Oxford Instruments, MercuryiTC) and a gas flow controller. For high-spin ferric heme, spectra were recorded at 10 K using the following parameters: 0.1 mW microwave power (no saturation), 100 kHz modulation frequency and 5 G modulation amplitude. For the radical signal, spectra were recorded at 50 K due to its slower relaxation property compared to ferric heme using the following parameters of 0.1 mW microwave power (no saturation), 100-kHz modulation frequency and 5 G modulation amplitude. Q-band (approximately 34.0 GHz) ^{1}H Davies ENDOR experiments were performed on a Bruker Biospin EleXsys 580 spectrometer equipped with a 10 W amplifier and an R.A. Isaacson cylindrical TE_{011} resonator in an Oxford CF935 cryostat at the University of California, Davis. ENDOR measurements of the radical signal were carried out at 50 K by employing Davies pulse sequence (π–RF–π/2–τ–π–τ–echo) for large hyperfine couplings[44]. ENDOR spectrum was collected stochastically by randomly hopping the radiofrequency excitation frequency[45]. Pulse sequences were programmed with the PulseSPEL programmer via the Xepr interface. Simulations of the continuous-wave spectra and the following pulse EPR spectra were performed using the EasySpin 5.2.35 toolbox[46,47] within the MATLAB 2014a software suite (MathWorks). The simulation uses the $[g_x, g_y, g_z]$ = [2.0060, 2.0040, 2.0030] and three ^{1}H hyperfine tensors: $A(^1H7_a)$ = [18, 22, 23] MHz, $A(^1H5)$ = [14, 17, 17] MHz and $A(^1H3)$ = [14, 17, 17] MHz. The hyperfine coupling for ^{1}H7b, ^{1}H2 and ^{1}H6 are in the range of <10 MHz.

Assessment of APEX2's photoreactivity in an anaerobic glovebox

DPBS and BN2 were transferred into the anaerobic N2 gas-filled glovebox for more than 24 hours to ensure complete removal of dissolved O_2. Purified APEX2 (36 µM in DPBS) was then introduced into the anaerobic box, and its buffer was exchanged with anaerobic DPBS using 10-kDa molecular weight cutoff (MWCO) ultrafiltration tubes. The buffer exchange was performed three times by centrifugation at 12,000 r.p.m. for 5 minutes each, with room lights turned off throughout the process. BN2 (500 µM) and APEX2 were mixed in the glovebox. To assess the effect of blue light exposure on the BN2–APEX2 mixture, an LED lamp (410 nm, 34 mW cm^{-2}) was placed inside the glovebox and used to illuminate the mixture for 5 minutes. After the reaction, 5× protein loading buffer was added to quench the reaction. Samples were then analyzed by western blotting to evaluate BN2 labeling of APEX2 under either anaerobic or aerobic conditions.

In vitro activity test of APEX2 and its mutants

APEX2 or its mutants (1 µg $µl^{-1}$) were mixed with BN2 (500 µM), and the reaction was initiated by adding blue light at the specified intensity, duration and concentration. After the reaction, protein loading buffer was immediately added to stop the reaction, and the samples were stored for subsequent western blotting analysis without being boiled (avoid heat-induced labeling). The PVDF membrane with the blotted samples was probed for labeling signals using a streptavidin–HRP antibody. Equal loading of samples was confirmed by Coomassie blue staining.

Reporting summary

Further information on research design is available in the Nature Portfolio Reporting Summary linked to this article.

Data availability

All data are available in the main text or the supplementary materials. All the raw MS data have been deposited in the ProteomeXchange with identifier PXD064195. The X-ray crystallography data of APEX2 have been uploaded to the PDB with visiting accession ID 9KOE. Source data are provided with this paper.

References

44. Davies, E. R. A new pulse endor technique. *Phys. Lett.* **47**, 1–2 (1974).
45. Bruggemann, W. & Niklas, J. R. Stochastic ENDOR. *J. Magn. Reson.* **108**, 25–29 (1994).
46. Stoll, S. & Schweiger, A. EasySpin, a comprehensive software package for spectral simulation and analysis in EPR. *J. Magn. Reson.* **178**, 42–55 (2006).
47. Stoll, S. & Britt, R. D. General and efficient simulation of pulse EPR spectra. *Phys. Chem. Chem. Phys.* **11**, 6614–6625 (2009).

Acknowledgements

We appreciate the support of the Tsinghua University Technology Center for the X-ray crystallography facility. We thank R. D. Britt for his support with the access of the Q-band pulse ^{1}H ENDOR EPR instrument (University of California, Davis) and experiments. We thank the staff members of the Biological Mass Spectrometry System at the Dalian Coherent Light Source for providing technical support and assistance in data collection and analysis. The authors thank P. Zou (Peking University) and S. GongJin for their kind assistance with APEX2–OMM labeling and imaging. The authors also thank J. Zheng, W. Gao, Y. Mao, T. Yan, K. Zhang and Y. Liang for their valuable advice and experimental assistance. The authors acknowledge funding from the National Natural Science Foundation of China (22125403, R.T.; 92253304, R.T.; 92353301, X.Y.; 91953118, R.T.; 92359302, R.T.; 8234100284, R.T.; 2201218, R.T.); the China State Key Basic Research Program (2024YFA1307200, R.T.; 2021YFA1301601, R.T.; 2022YFC3401100, Z.D.; 2021YFA1301602, R.T.; SQ2024AAA030643, R.T.; 2023ZD0509501, L.T.; 2021YFA1302603, R.T.); the China Postdoctoral Science Foundation (2024M761287, M.K.); and the Shenzhen Innovation of Science and Technology Commission (ZDSYS20230626090803004, R.T.; KJZD20230923114220041, R.T., 20231120094247002, L.T.).

Author contributions

R.T. conceived the project, with the collaboration of L.T. for mechanistic study and Z.L. for generating the mouse model. R.T., L.T. and M.K. managed and designed the experiments. M.K. and F.L. performed most of the experiments. A.H. designed and synthesized the probes. G.W. constructed and raised the mice. M.K. and A.H. analyzed the data. L.T., B.M., Z.T. and A.H. performed the EPR experiments and analysis as well as the nuclear magnetic resonance analysis of the BN2–histidine conjugation. Z.L., F.W. and X.Y. performed UVPD–MS analysis. Y.X. and Y.L. supported the PHx surgery. J.W. and Z.D. supported the mechanism study. Z.Z. helped with the tissue slice experiments. P.S. and K.H. assisted with confocal imaging of mitochondrial morphology. R.T., L.T. and M.K. wrote the manuscript.

Competing interests

The authors declare no competing interests.

Additional information

Extended data is available for this paper at https://doi.org/10.1038/s41589-026-02230-0.

Supplementary information The online version contains supplementary material available at https://doi.org/10.1038/s41589-026-02230-0.

Correspondence and requests for materials should be addressed to Zhiyong Liu, Lizhi Tao or Ruijun Tian.

Peer review information *Nature Chemical Biology* thanks the anonymous reviewers for their contribution to the peer review of this work.

https://doi.org/10.1038/s41589-026-02230-0

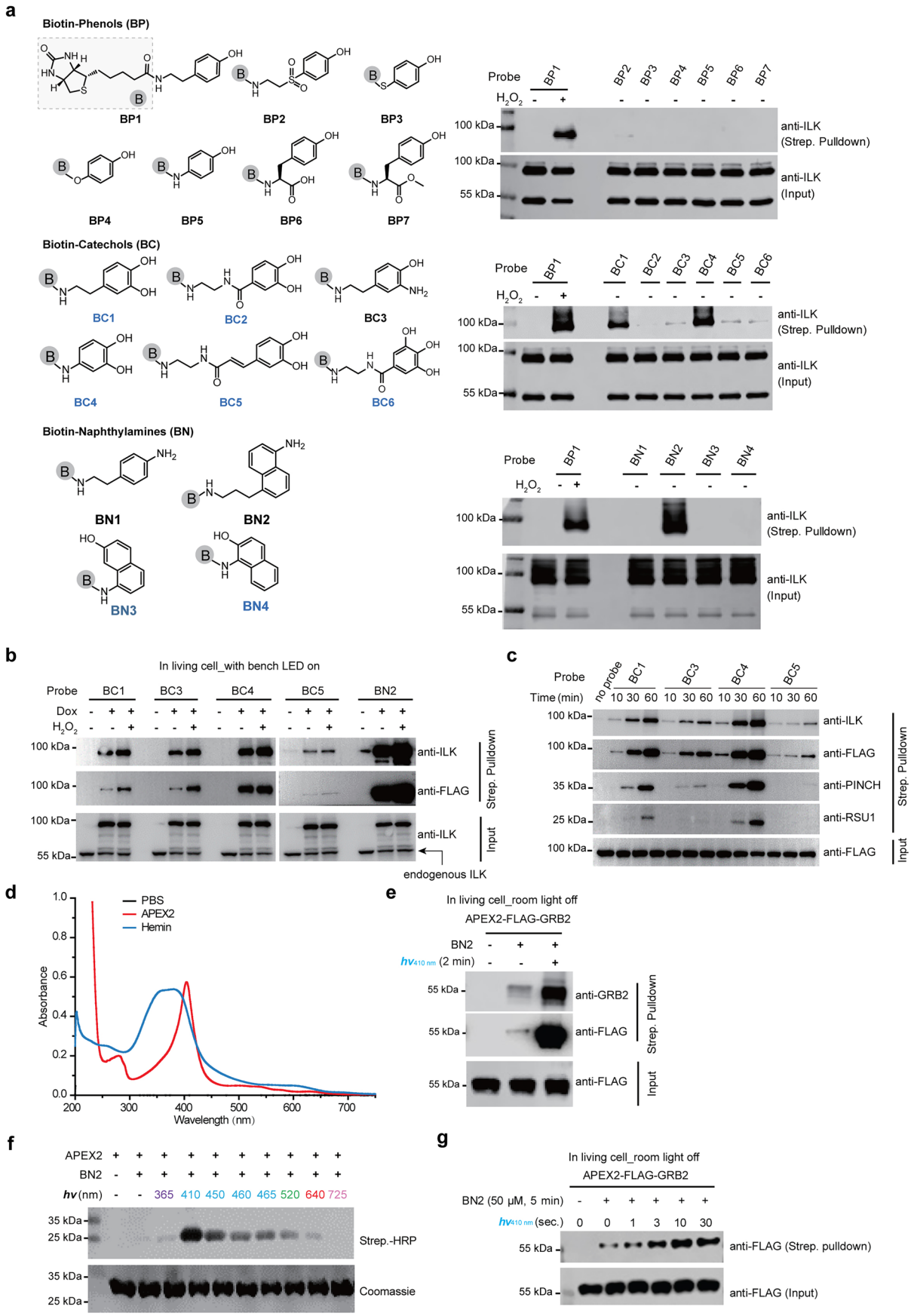

Extended Data Fig. 1 | See next page for caption.

https://doi.org/10.1038/s41589-026-02230-0

Extended Data Fig. 1 | Related to Fig. 1. a, Analysis of structures and activities of 6 Biotin-Phenol analogs, 6 Biotin-Catechol analogs, and 4 Biotin-Naphthylamine analogs. The probes highlighted in blue are introduced in this work, while the others are derived from our previous study. Each probe was incubated with cells stably expressing ILK fused with N-terminal APEX2-FLAG for 10 minutes (biological replicates $n = 3$). The room light was on during the experiments. **b**, Activity analysis of the five probes that show reactivity in the H_2O_2-free screening, with 500 μM H_2O_2 as the positive control. **c**, Western blot analysis of the labeling performance of BC1, BC3, BC4, and BC5 on the IPP-RSU1 protein complex, with probe incubation times of 30 or 60 minutes (biological replicates $n = 3$). **d**, UV-Visible absorbance of APEX2 and hemin. **e**, BN2–APEX2 was tested about its photoreactivity in living cells. BN2 was incubated with living cells at 50 μM for 2 minutes with/without blue light exposure (biological replicates $n = 3$). **f**, Photoreactivity of APEX2 and BN2 under LED light irradiation at different wavelengths. Samples were exposed to light for 2 minutes (biological replicates $n = 3$). **g**, BN2 labeling of APEX2-FLAG tagged GRB2 in living cells, triggered by indicated seconds resolution of blue light exposure (biological replicates $n = 3$).

https://doi.org/10.1038/s41589-026-02230-0

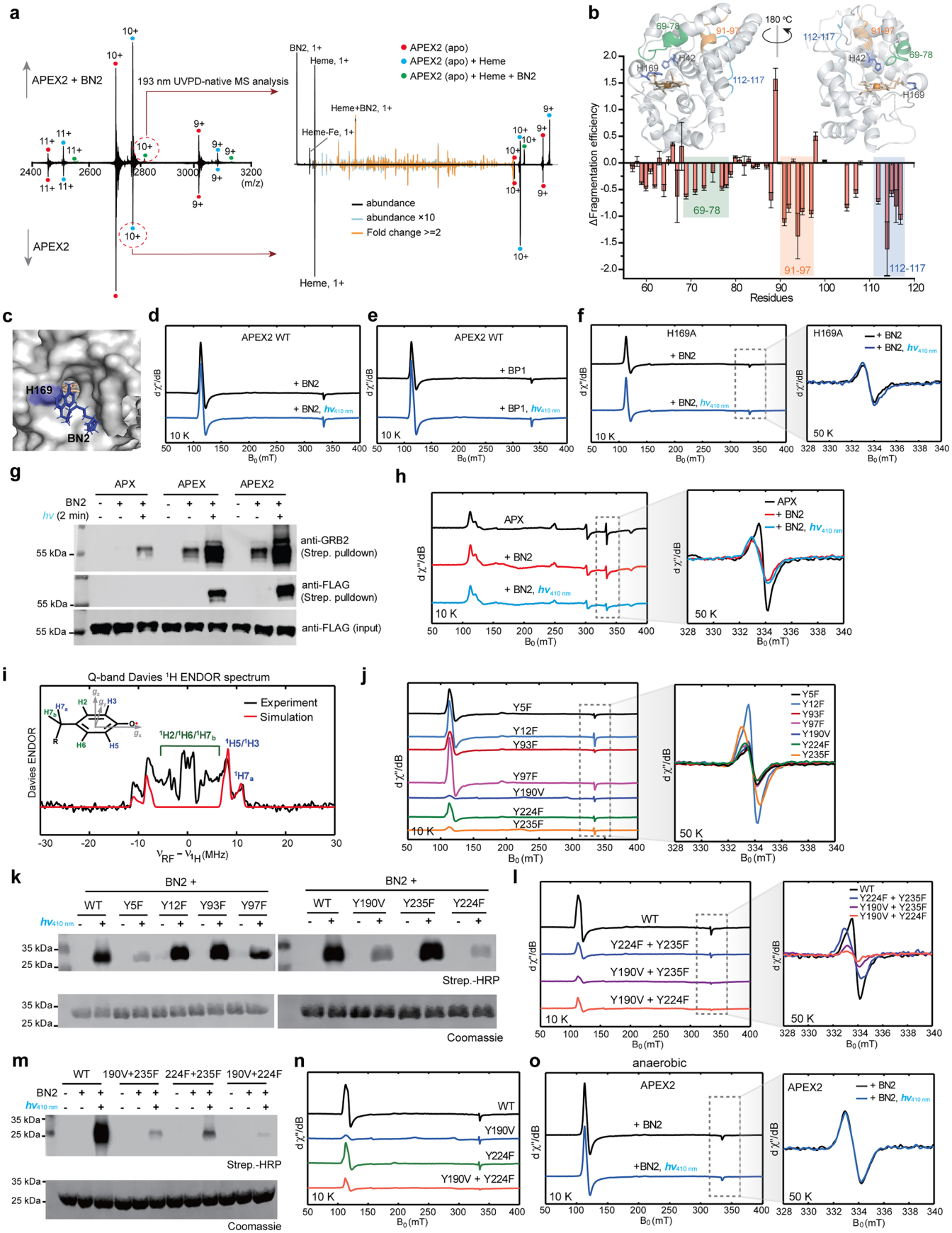

Extended Data Fig. 2 | See next page for caption.

https://doi.org/10.1038/s41589-026-02230-0

Extended Data Fig. 2 | Related to Fig. 2. a, Native MS spectrum of APEX2 in the presence of BN2, accompanied by 193 nm UVPD-tandem MS fragmentation. **b**, Delta fragmentation efficiency analysis of APEX2 with or without BN2. See the full data in Supplementary Table 2. Regions with consecutive 5 positions showing Δ fragmentation efficiency < − 0.3 (ignore the 0 value) are shadowed and labeled in the APEX2 structure. **c**, The naphthylamine group of BN2 was modeled into this electron density, resulting in the presented model. **d**, X-band CW EPR spectra (at 10 K) of APEX2 upon addition of BN2 or excitation at 410 nm under aerobic condition. **e**, X-band CW EPR spectra of APEX2 upon addition of BP1 or excitation at 410 nm under aerobic condition at 10 K. **f**, X-band CW EPR spectra reveal radical signatures of the H169A mutant following BN2 and blue light treatment. **g**, Photo-reactivity of APX/ APEX/ APEX2 combined with BN2 (biological replicates $n = 3$) in HeLa cells. Labeling was performed using 50 μM BN2 under blue light illumination for 2 minutes. **h**, X-band CW EPR spectra of APX upon addition of BN2 or excitation at 410 nm under aerobic condition at 10 K and 50 K. **i**, Q-band (34.1255 GHz) ^{1}H ENDOR EPR spectrum of APEX2 recorded at 1215.9 mT with $g = 2.0052$. **j**, X-band CW EPR spectra show radical signals in the seven single tyrosyl mutants at 10 K (left) and 50 K (right). **k**, Assessment of photoreactivity by exposing the tyrosine mutants with BN2 to blue light for 5 minutes (biological replicates $n = 3$). **l**, X-band CW EPR spectra of APEX2 and the double tyrosine mutants at 10 K (left) and 50 K (right). **m**, Photoreactivity analysis of the double tyrosine mutants (biological replicates $n = 3$). **n**, X-band CW EPR spectra of APEX2 and the indicated single or double tyrosine mutants at 10 K. **o**, X-band CW EPR spectra of APEX2 upon addition of BN2 or excitation at 410 nm under anaerobic condition.

https://doi.org/10.1038/s41589-026-02230-0

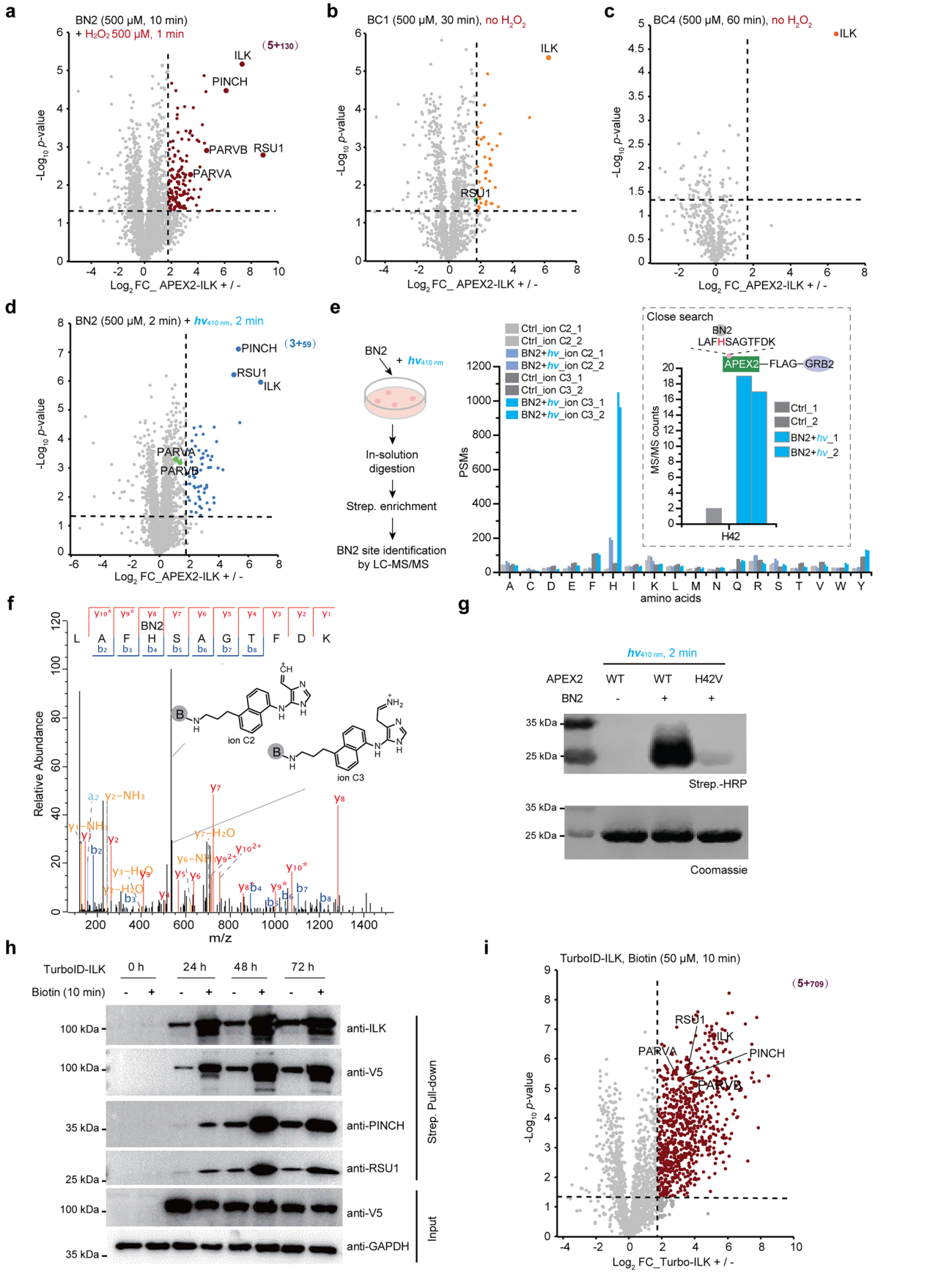

Extended Data Fig. 3 | See next page for caption.

https://doi.org/10.1038/s41589-026-02230-0

Extended Data Fig. 3 | Related to Fig. 3. a, Volcano plots depicting the AP-MS results for the IPP-RSU1 complex labeled with 500 µM BN2 and 500 µM H_2O_2 for 1 minutes (Biological replicates $n = 3$, $Log_2FC > 1.8$, p-value < 0.05, two-sided student's test, no adjustments). **b-c**, Volcano plot showing BC1-mediated PL of the IPP-RSU1 complex, with 500 µM BC1 incubated with cell for 30 minutes (**b**), and with 500 µM BC4 incubated with cell for 60 minutes (**c**) (biological replicates $n = 3$ for the $APEX2^-$ group and $n = 4$ for the $APEX2^+$ group, $Log_2FC > 1.8$, p-value < 0.05, two-sided student's test, no adjustments). **d**, Volcano plot depicting the AP-MS results for the IPP-RSU1 complex labeled with 500 µM BN2 and exposed to 410 nm light for 2 minutes (biological replicates $n = 3$, $Log_2FC > 1.8$, p-value < 0.05, two-sided student's test, no adjustments). Both $APEX2^+$ and $APEX2^-$ groups were treated with the indicated probe concentrations and exposed to light for the specified durations. **e**, Analysis of BN2's preferred labeling sites through examining BN2-labeled protein digests in living cells (biological replicates $n = 2$). **f**, MS2 spectrum showing BN2 modification on the H42 residue in APEX2. **g**, Labeling effects were examined for H42 mutants in which histidine was substituted with valine (V) (biological replicates $n = 3$). **h**, Western blot analysis of TurboID-based PL of the IPP-RSU1 complex. HT1080 cells stably transfected with doxycycline-inducible TurboID-V5-tagged ILK were incubated with 50 µM biotin for 10 minutes or left untreated (biological replicates $n = 3$). **i**, Proteomic analysis of TurboID-mediated PL of the IPP-RSU1 complex, showing the detection and quantification of the IPP-RSU1 components. $Turbo^+$ and $Turbo^-$ groups were both treated with 50 µM biotin for 10 minutes. (biological replicates $n = 3$ for the $Turbo^-$ group and $n = 4$ for the $Turbo^+$ group, $Log_2FC > 1.8$, p-value < 0.05, two-sided student's test, no adjustments).

https://doi.org/10.1038/s41589-026-02230-0

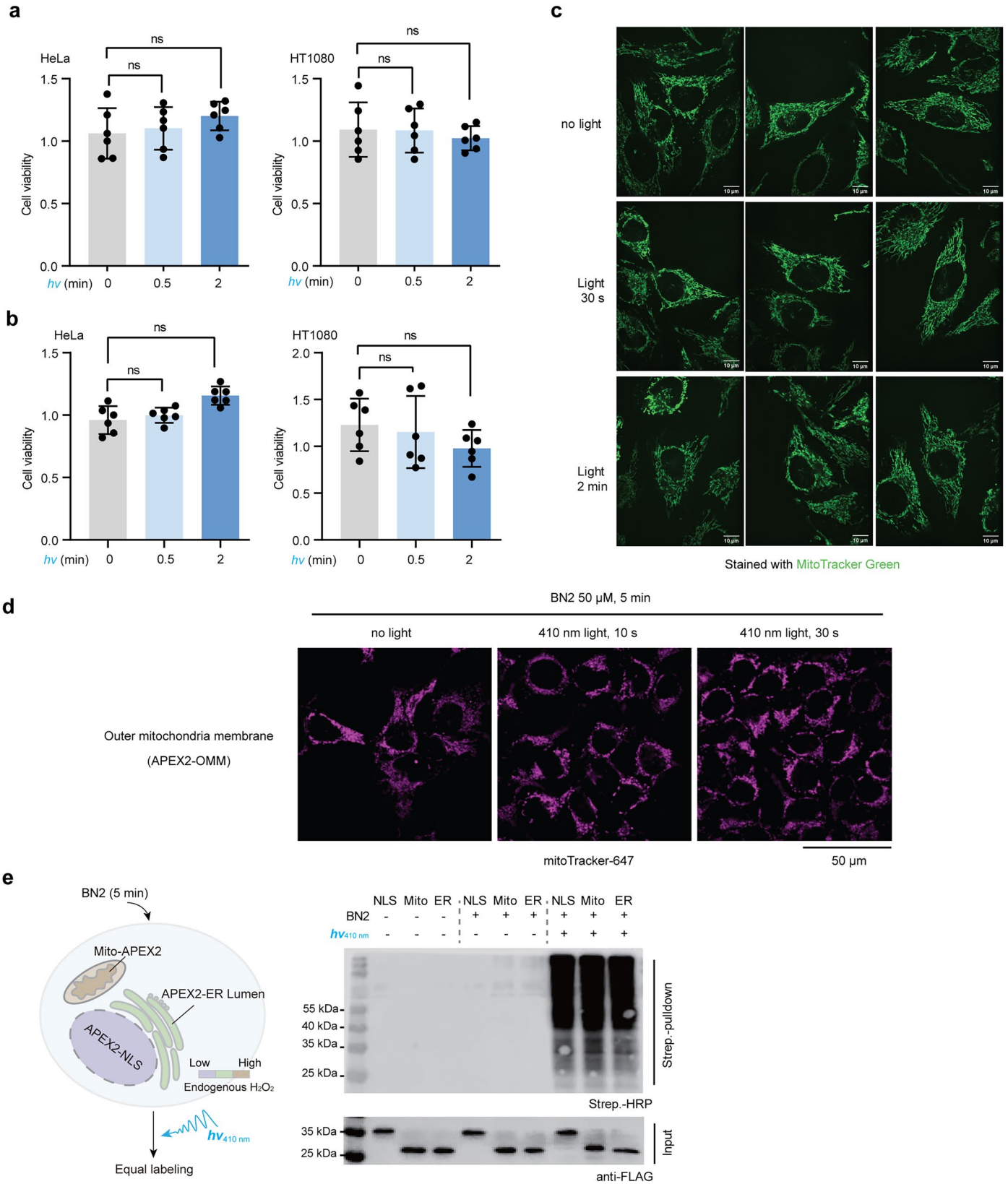

Extended Data Fig. 4 | See next page for caption.

https://doi.org/10.1038/s41589-026-02230-0

Extended Data Fig. 4 | Related to Fig. 3. a, CellTiter96 assay measuring viability of HeLa and HT1080 cells after 410 nm light exposure for 30 seconds or 2 minutes (biological replicates $n = 6$), data are presented as mean values +/− SEM. **b**, CCK-8 assay assessing cell viability of HeLa and HT1080 cells under the same light exposure conditions (biological replicates $n = 6$), data are presented as mean values +/− SEM. **c**, Confocal microscopy images showing mitochondrial morphology following light exposure. Mitochondria of HeLa cell were stained with MitoTracker Green and imaged live using a spinning-disk confocal microscope (biological replicates $n = 3$). The scale bar is 10 µm. **d**, Confocal microscopy images showing mitochondrial morphology following complete ROProx labeling in HEK293T cells expressing APEX2-OMM. Cells were treated with 50 µM BN2 for 5 minutes and subjected to 410 nm light (34 mW/cm^2) for the final 10 seconds or 30 seconds, as indicated (biological replicates $n = 3$). **e**, Comparison of light-dependent labeling at different subcellular spaces without external H_2O_2. Cells expressing APEX2-FLAG-tagged subcellular signal peptides were treated with 50 µM BN2 for 5 minutes or along with blue light exposure for 5 minutes (biological replicates $n = 3$).

https://doi.org/10.1038/s41589-026-02230-0

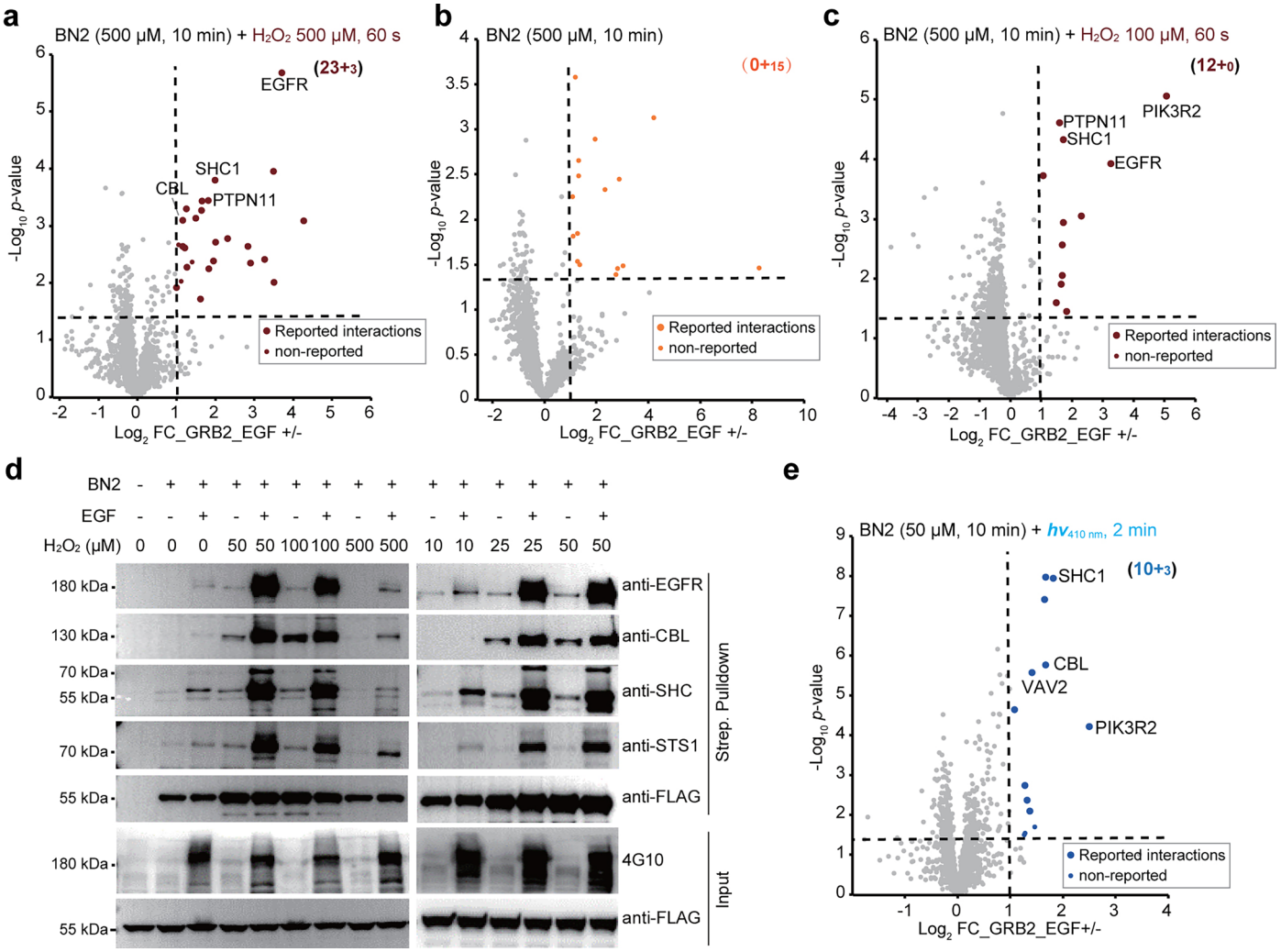

Extended Data Fig. 5 | Related to Fig. 4. a, Proteomic analysis of BN2's performance in labeling the EGF-stimulated GRB2 interactome with 500 μM H_2O_2 treatment for 1 minute. BN2 (500 μM) was applied for 10 minutes, with EGF added 2 minutes before cell harvest and H_2O_2 added at the last minute. **b**, Proteomic analysis of BN2's performance in labeling the EGF-stimulated GRB2 interactome without H_2O_2 treatment. BN2 (500 μM) was applied for 10 minutes, with EGF added 2 minutes before cell harvest. **c**, Proteomic analysis of BN2's performance in labeling the EGF-stimulated GRB2 interactome with 100 μM H_2O_2 treatment. BN2 (500 μM) was applied for 10 minutes. For **a**, **b**, and **c**, biological replicates $n = 3$ for EGF- and EGF+ group respectively, $Log_2FC > 1$ and p-value < 0.05, two-sided student's test, no adjustments. **d**, Western blot to explore the potentiality of BN2 in labeling dynamic protein complex under varying concentrations of H_2O_2 (biological replicates $n = 3$). The concentration of BN2 was 50 μM, and the incubation time was 10 minutes. EGFR, CBL, SHC, and STS1 are known interacting proteins of GRB2 upon EGF stimulation. **e**, Volcano plot of AP-MS results for IPP-RSU1 complex labeled with 50 μM BN2 plus blue light exposure for 2 min (biological replicates n = 4, $Log_2FC > 1$ and p-value < 0.05, two-sided student's test, no adjustments).

https://doi.org/10.1038/s41589-026-02230-0

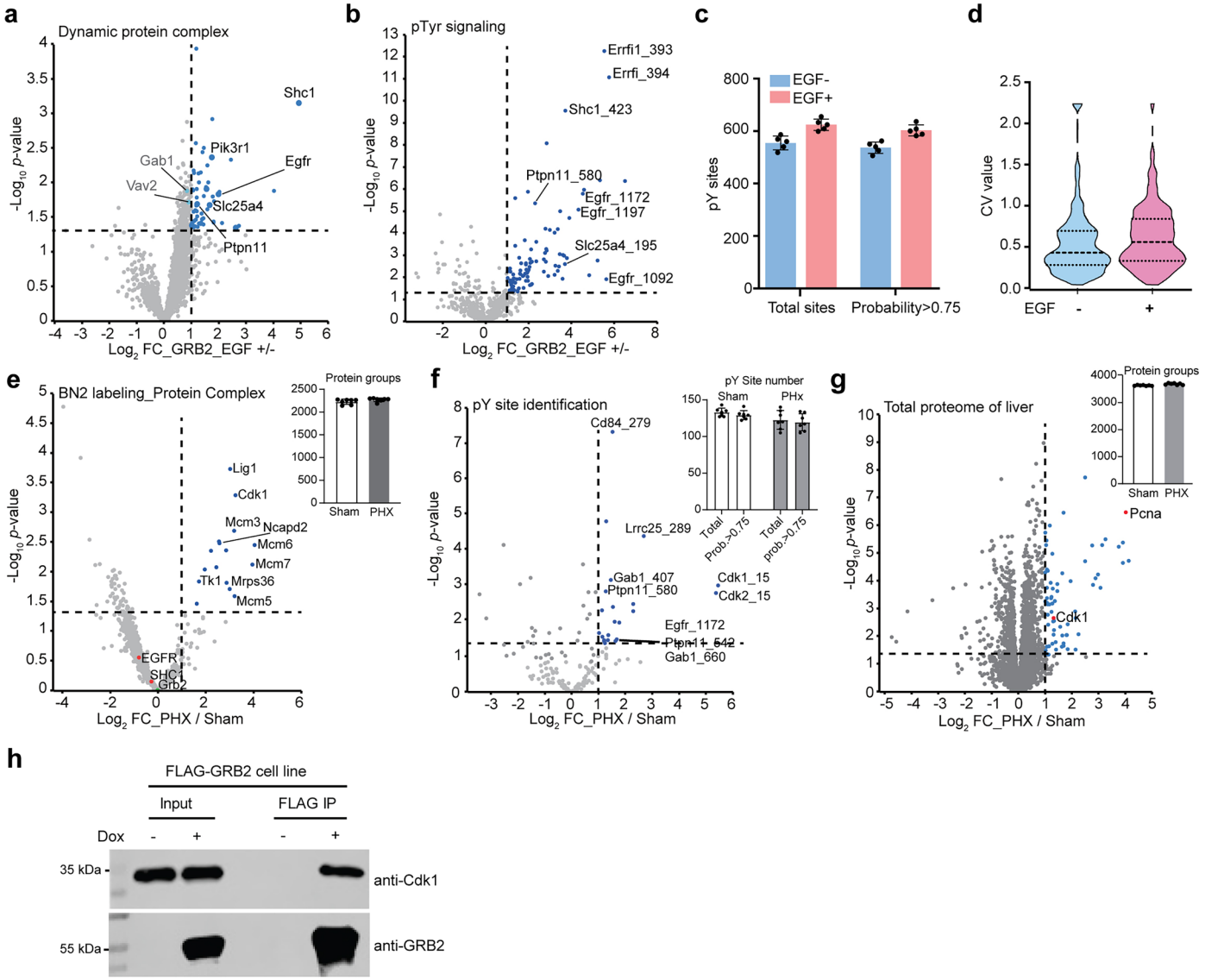

Extended Data Fig. 6 | Related to Fig. 6. a, Volcano plot of the EGF-stimulated Grb2 interactome. Proteins with $Log_2FC > 1$ and p-value < 0.05 are marked in blue, with known interacting proteins annotated (two-sided student's test, no adjustments). The samples are the same as in the pTyr proteome analysis (EGF-, $n = 5$; EGF + , $n = 5$). **b**, Volcano plot of the stimulated pTyr proteome in mouse liver following EGF stimulation (EGF-, $n = 5$; EGF + , $n = 5$). Sites with $Log_2FC > 1$ and p-value < 0.05 are marked in blue, with selected sites annotated (two-sided student's test, no adjustments). Duplicate samples were collected from each mouse, providing ten data points for each group. **c**, Number of pTyr sites identified in the EGF stimulated liver tissue, data are presented as mean values +/− SEM. **d**, CV distribution of identified pTyr peptide intensities in samples before and after EGF stimulation. For the box plots, the central line indicates the median, the box bounds represent the 25th to 75th percentiles, and the whiskers extend to the minimum and maximum values. **e-g**, ROProx identified Grb2 interactome (**e**), volcano plot of the BN2-mediated PL of pTyr sites (**f**), and total proteome (**g**) of liver identified in the PHx group vs. Sham group (PHx $n = 7$, Sham $n = 7$). Sites or proteins with $Log_2FC > 1$ and p-value < 0.05 are marked with blue dots, with some specific proteins marked with names (two-sided student's test, no adjustments). **h**, Validation of the interaction between Grb2 and Cdk1 using IP-WB of CDK1 in cell line (biological replicates $n = 4$). Doxycycline was added to induce FLAG-tagged Grb2 expression.

nature portfolio

Corresponding author(s): Ruijun Tian

Last updated by author(s): Mar 25, 2026

Reporting Summary

Nature Portfolio wishes to improve the reproducibility of the work that we publish. This form provides structure for consistency and transparency in reporting. For further information on Nature Portfolio policies, see our Editorial Policies and the Editorial Policy Checklist.

Statistics

For all statistical analyses, confirm that the following items are present in the figure legend, table legend, main text, or Methods section.

n/a	Confirmed
☐	☒ The exact sample size (*n*) for each experimental group/condition, given as a discrete number and unit of measurement
☐	☒ A statement on whether measurements were taken from distinct samples or whether the same sample was measured repeatedly
☐	☒ The statistical test(s) used AND whether they are one- or two-sided *Only common tests should be described solely by name; describe more complex techniques in the Methods section.*
☒	☐ A description of all covariates tested
☐	☒ A description of any assumptions or corrections, such as tests of normality and adjustment for multiple comparisons
☐	☒ A full description of the statistical parameters including central tendency (e.g. means) or other basic estimates (e.g. regression coefficient) AND variation (e.g. standard deviation) or associated estimates of uncertainty (e.g. confidence intervals)
☐	☒ For null hypothesis testing, the test statistic (e.g. *F*, *t*, *r*) with confidence intervals, effect sizes, degrees of freedom and *P* value noted *Give P values as exact values whenever suitable.*
☒	☐ For Bayesian analysis, information on the choice of priors and Markov chain Monte Carlo settings
☐	☒ For hierarchical and complex designs, identification of the appropriate level for tests and full reporting of outcomes
☒	☐ Estimates of effect sizes (e.g. Cohen's *d*, Pearson's *r*), indicating how they were calculated

Our web collection on statistics for biologists contains articles on many of the points above.

Software and code

Policy information about availability of computer code

Data collection	The MS data were collected using Thermo Scientific Xcalibur software (version 4.1.50). All WB images were collected using a Tanon 6100C (SN14T15RGBFLI6-1226) or Odyssey FC imaging system. Confocal images were acquired using the Micro-Manager (version 2.0) software. The EPR data were collected using the Xepr (version 1.0) software.
Data analysis	All the raw files were searched in MaxQuant software (version 1.5.5.1). Data processing, statistical analysis, and data visualization were conducted using R software (version 3.6.2), Perseus (version 1.5.5.3), Origin (version 8.0), and GraphPad Prism (version 9.5).

For manuscripts utilizing custom algorithms or software that are central to the research but not yet described in published literature, software must be made available to editors and reviewers. We strongly encourage code deposition in a community repository (e.g. GitHub). See the Nature Portfolio guidelines for submitting code & software for further information.

Data

Policy information about availability of data

All manuscripts must include a data availability statement. This statement should provide the following information, where applicable:

- Accession codes, unique identifiers, or web links for publicly available datasets
- A description of any restrictions on data availability
- For clinical datasets or third party data, please ensure that the statement adheres to our policy

All data are available in the main text or the supplementary materials. All the raw MS data have been deposited in the ProteomeXchange with identifier PXD064195.

Reviewers can access the dataset by logging in to the PRIDE website using the following account details: Username: reviewer_pxd064195@ebi.ac.uk, Password: wNnX9OJNp7sC (alternatively, reviewers can access the MS raw data through the accession: PXD064195 and Token: H5UrBr9GkiOt). The X-ray crystallography data of APEX2 has been uploaded to the protein data bank (RCSB PDB) with a visiting accession ID 9KOE. The ChemDraw files, EPR raw data, Uncropped im-ages of the biological replications etc. can be found in the Source data file.

Research involving human participants, their data, or biological material

Policy information about studies with human participants or human data. See also policy information about sex, gender (identity/presentation), and sexual orientation and race, ethnicity and racism.

Reporting on sex and gender	*Use the terms sex (biological attribute) and gender (shaped by social and cultural circumstances) carefully in order to avoid confusing both terms. Indicate if findings apply to only one sex or gender; describe whether sex and gender were considered in study design; whether sex and/or gender was determined based on self-reporting or assigned and methods used. Provide in the source data disaggregated sex and gender data, where this information has been collected, and if consent has been obtained for sharing of individual-level data; provide overall numbers in this Reporting Summary. Please state if this information has not been collected. Report sex- and gender-based analyses where performed, justify reasons for lack of sex- and gender-based analysis.*
Reporting on race, ethnicity, or other socially relevant groupings	*Please specify the socially constructed or socially relevant categorization variable(s) used in your manuscript and explain why they were used. Please note that such variables should not be used as proxies for other socially constructed/relevant variables (for example, race or ethnicity should not be used as a proxy for socioeconomic status). Provide clear definitions of the relevant terms used, how they were provided (by the participants/respondents, the researchers, or third parties), and the method(s) used to classify people into the different categories (e.g. self-report, census or administrative data, social media data, etc.) Please provide details about how you controlled for confounding variables in your analyses.*
Population characteristics	*Describe the covariate-relevant population characteristics of the human research participants (e.g. age, genotypic information, past and current diagnosis and treatment categories). If you filled out the behavioural & social sciences study design questions and have nothing to add here, write "See above."*
Recruitment	*Describe how participants were recruited. Outline any potential self-selection bias or other biases that may be present and how these are likely to impact results.*
Ethics oversight	*Identify the organization(s) that approved the study protocol.*

Note that full information on the approval of the study protocol must also be provided in the manuscript.

Field-specific reporting

Please select the one below that is the best fit for your research. If you are not sure, read the appropriate sections before making your selection.

☒ Life sciences ☐ Behavioural & social sciences ☐ Ecological, evolutionary & environmental sciences

For a reference copy of the document with all sections, see nature.com/documents/nr-reporting-summary-flat.pdf

Life sciences study design

All studies must disclose on these points even when the disclosure is negative.

Sample size	To ensure the reliability and quantification precision; all experiments are performed with at least three biological replicates. For the in vivo quantitative analysis of Grb2 interacting proteins upon EGF stimulation, n=5 mice were used for control and EGF group respectively; for the analysis of Grb2's interactome during liver regeneration, n=7 mice were used for the Sham and PHx group respectively.
Data exclusions	In each label-free quantification process, the proteins in the "proteingroups" table marked with "identified only by site", "potential contamination" and "reverse" are excluded at the beginning of the analysis. No other data are excluded.
Replication	All the data are done with at least three biological replicates except that the following figures are based on two biological replicates: Fig. 3e and Extended Data Fig. 3e, Fig. 3g, and Fig. 4f. Our scientific justifications are as follows: (1) For Fig. 3e, two in vitro biological replicates identified 296 and 339 BN2-modified PSMs, respectively. In Extended Data Fig. 3e, proximity labeling in living cells yielded ~1,000 BN2–His fragment ions in each of the two biological replicates. Together, these independent experiments consistently confirm BN2 modification on histidine residues of proximal proteins, particularly at the H42 site of APEX2, and cross-validate each other. (2) In Fig. 3g, two biological replicates consistently demonstrate the dominant labeling activity of APEX2 in combination with BN2. This observation is further supported by an independent proteomics dataset comparing APEX2 + BN2, LOV-Turbo + biotin, and miniSOG + BN1 using a different bait protein (n = 3 biological replicates per condition; data provided in the rebuttal but not included in the manuscript; the data is available upon request.). Moreover, pulldown–WB analysis from two biological replicates showed that miniSOG + biotin-NH2 exhibited minimal labeling activity relative to the other methods; accordingly, its proteomic performance was not further evaluated. (3) For Fig. 4f, the conclusion is independently corroborated by the mass spectrometry results in Fig. 4e. For the quantitative analysis of Grb2 interacting proteins upon EGF stimulation, n=5 mice were used for control and EGF group respectively; for the analysis if Grb2's interactome during liver regeneration, n=7 mice were used for the Sham and PHx group respectively.
Randomization	The mice were randomly allocated for the experiments.

Blinding

In our work, cell lines and mice were used. Cell lines were not blinding to the performers. Mice were identified expressing the APEX2-FLAG tagged Grb2, and then randomly allocated for the following experiments. We included all the data for analysis.

Reporting for specific materials, systems and methods

We require information from authors about some types of materials, experimental systems and methods used in many studies. Here, indicate whether each material, system or method listed is relevant to your study. If you are not sure if a list item applies to your research, read the appropriate section before selecting a response.

Materials & experimental systems

n/a	Involved in the study
☐	☒ Antibodies
☐	☒ Eukaryotic cell lines
☐	☐ Palaeontology and archaeology
☐	☒ Animals and other organisms
☐	☐ Clinical data
☐	☐ Dual use research of concern
☐	☐ Plants

Methods

n/a	Involved in the study
☐	☐ ChIP-seq
☐	☐ Flow cytometry
☐	☐ MRI-based neuroimaging

Antibodies

Antibodies used

The primary and secondary antibodies used in this study included: 4G10 (Merk Millipore, 05-321, 1:1000), anti-pEGFR (Tyr1068) (CST, 3777s, 1:1000), anti-EGFR (CST, 4267s, 1:1000), anti-FLAG (SIGMA, F1804, 1:1000), anti-FLAG (CST, 14793, 1:1000), anti-GRB2 (BD, 610112, 1:2000), anti-SHC (BD, 610878, 1:2000), anti-CBL (CST, 8447, 1:1000), anti-STS1 (Abcam, ab34781, 1:1000), anti-GAPDH (Beyotime, AF0006, 1:1000). Streptavidin-HRP (Meilunbio, MB4748-2, 1:5000), anti-V5 (Merck, v8012, 1:1000), anti-ILK (CST, 3856s, 1:1000), anti-PINCH (BD, 612711, 1:1000), anti-RSU1 (Novus, NBP1-54879, 1:1000), anti-HA (CST, 3724T, 1:1000), anti-SLC25A4 (SIGMA, SAB2108761, 1:1000), anti-CDK1 (Beyotime, AF0111, 1:500), anti-CDK1 (MCE, HY-P80611, 1:500) and anti-CDK1 pY15 (MCE, HY-P80796, 1:500). The secondary antibodies include HRP-conjugated anti-rabbit (Beyotime, A0208, 1:1500) and anti-mouse (Beyotime, A0216, 1:1500).

Validation

All the primary antibodies used in this study are commercially available and widely used, and were assessed for expected molecular weight (western blot).
1. mouse 4G10: Merck Millipore, catalog number 05-321, Lot number 3433888. (dilution 1:1000) (https://www.merckmillipore.com/CN/zh/product/Anti-Phosphotyrosine-Antibody-clone-4G10,MM_NF-05-321?ReferrerURL=https%3A%2F%2Fcn.bing.com%2F)
2. Rabbit anti-pEGFR (Tyr1068): CST, catalog number 3777S, Lot number 16. (dilution 1:1000) (https://www.cellsignal.com/products/primary-antibodies/phospho-egf-receptor-tyr1068-d7a5-xp-rabbit-mab/3777?site-search-type=Products&N=4294956287&Ntt=3777s&fromPage=plp&_requestid=449261)
3. Rabbit anti-EGFR: CST, catalog number 4267, Lot number 19. (dilution 1:1000) (https://www.cellsignal.com/products/primary-antibodies/egf-receptor-d38b1-xp-rabbit-mab/4267?site-search-type=Products&N=4294956287&Ntt=4267s&fromPage=plp&_requestid=450098)
4. mouse anti-FLAG: SIGMA, catalog number F1804, Lot number SLCD3524. (dilution 1:1000) (https://www.sigmaaldrich.com/catalog/product/sigma/f1804?lang=zh&region=CN); CST, 14793 (dilution 1:1000) (https://www.cellsignal.com/products/primary-antibodies/dykddddk-tag-d6w5b-rabbit-monoclonal-antibody-binds-to-same-epitope-as-sigma-aldrich-anti-flag-m2-antibody/14793)
5. mouse anti-GRB2: BD, catalog number 610112, Lot number 4199954. (dilution 1:2000) (https://www.bdbiosciences.com/us/applications/research/b-cell-research/intracellular-antigens/human/purified-mouse-anti--grb2-81grb2/p/610112)
6. mouse anti-SHC: BD, catalog number 610878, Lot number 8025664.(dilution 1:2000) (https://www.bdbiosciences.com/us/reagents/research/antibodies-buffers/cell-biology-reagents/cell-biology-antibodies/purified-mouse-anti-shc-30shc/p/610878)
7. mouse anti-GAPDH: Beyotime, AF0006 (dilution 1:1000) (https://www.beyotime.com/product/AF0006.htm)
8. Streptavidin-HRP: Meilunbio, catalog number MB4748-2 (dilution 1:5000) (https://www.meilunbio.com/product/mb4748/)
9. anti-V5: Merck, catalog number v8012 (dilution 1:1000) (https://www.sigmaaldrich.cn/CN/zh/product/sigma/v8012?msockid=39bcd9c3a02d692c00c8cdfaa12c68dc)
10. anti-ILK: CST, catalog number 3856s (dilution 1:2000) (https://www.cellsignal.jp/products/primary-antibodies/ilk1-4g9-rabbit-monoclonal-antibody/3856)
11. anti-PINCH: BD, 612711 (dilution 1:1000) (https://www.bdbiosciences.com/en-eu/products/reagents/western-blotting-and-molecular-reagents/western-blot-reagents/purified-mouse-anti-pinch.612711)
12. anti-RSU1: Novus, NBP1-54879 (dilution 1:1000) (https://www.novusbio.com/products/rsu1-antibody_nbp1-54879)
13. mouse anti-HA: CST, catalog number 3724T (dilution 1:1000) (https://www.cellsignal.com/products/primary-antibodies/ha-tag-c29f4-rabbit-monoclonal-antibody/3724)
14. Rabbit anti-STS1: Abcam, catalog number ab34781, Lot number GR278584-6. (dilution 1:1000) (https://www.abcam.com/sts1-antibody-ab34781.html)
15. Rabbit anti-CBL: CST, catalog number 8447, Lot number 1. (dilution 1:1000) (https://www.cellsignal.com/products/primary-antibodies/c-cbl-d4e10-rabbit-mab/8447?site-search-type=Products&N=4294956287&Ntt=8447s&fromPage =plp&_requestid =450371)
16. anti-SLC25A4: SIGMA, SAB2108761 (dilution 1:1000) (https://www.sigmaaldrich.cn/CN/zh/product/sigma/sab2108761)
17. anti-CDK1: Beyotime, AF0111 (dilution 1:500) (https://www.beyotime.com/product/AF0111.htm)
18. anti-CDK1: MCE, HY-P80611 (dilution 1:500) (https://www.medchemexpress.cn/antibody/cdk1-rabbit-mab.html)
19. anti-CDK1 pY15: MCE, HY-P80796 (dilution 1:500) (https://www.medchemexpress.cn/antibody/phospho-cdk1-tyr15-rabbit-pab.html)

20. HRP-conjugated Goat anti-rabbit: Beyotime, catalog number A0208. (dilution 1:1000) (https://www.beyotime.com/product/A0208.htm)
21. HRP-conjugated Goat anti-mouse: Beyotime, catalog number A0216. (dilution 1:1000). (https://www.beyotime.com/product/A0216.htm)

Eukaryotic cell lines

Policy information about cell lines and Sex and Gender in Research

Cell line source(s)	The original HEK 293T and HeLa cell lines were purchased from National Collection of Authenticated Cell Cultures cell bank. And the stable cell lines expressing specific tagged-protein were homemade based on the cell lines from National Collection of Authenticated Cell Cultures. HEK 293T (CSTR:19375.09.3101HUMGNHu44, https://www.cellbank.org.cn/search-detail.php?id=375); HeLa (CSTR:19375.09.3101HUMTCHu187, https://www.cellbank.org.cn/search-detail.php?id=105). The HEK293T APEX2-OMM cell line is gifted by Prof. Peng Zou's lab (Peking University); The HT1080 cell line was a gift from Prof. Chuanyue Wu's lab (Southern University of Science and Technology).
Authentication	All the cell lines from National Collection of Authenticated Cell Cultures were authenticated by STR profiling data exposed by National Collection of Authenticated Cell Cultures cell bank.
Mycoplasma contamination	All the cell lines were tested for Mycoplasma contamination by National Collection of Authenticated Cell Cultures and us when receiving the cell lines, and are reported negative contamination of Mycoplasma.
Commonly misidentified lines (See ICLAC register)	No.

Palaeontology and Archaeology

Specimen provenance	*Provide provenance information for specimens and describe permits that were obtained for the work (including the name of the issuing authority, the date of issue, and any identifying information). Permits should encompass collection and, where applicable, export.*
Specimen deposition	*Indicate where the specimens have been deposited to permit free access by other researchers.*
Dating methods	*If new dates are provided, describe how they were obtained (e.g. collection, storage, sample pretreatment and measurement), where they were obtained (i.e. lab name), the calibration program and the protocol for quality assurance OR state that no new dates are provided.*

☐ Tick this box to confirm that the raw and calibrated dates are available in the paper or in Supplementary Information.

Ethics oversight	*Identify the organization(s) that approved or provided guidance on the study protocol, OR state that no ethical approval or guidance was required and explain why not.*

Note that full information on the approval of the study protocol must also be provided in the manuscript.

Animals and other research organisms

Policy information about studies involving animals; ARRIVE guidelines recommended for reporting animal research, and Sex and Gender in Research

Laboratory animals	C57BL/6J mice (6-8 weeks old) were used for animal experiments.
Wild animals	No.
Reporting on sex	No.
Field-collected samples	Mice were housed in SPF-level an-imal rooms (2-6 mice per cage) with 12-hour light/dark cycles in pathogen-free conditions, with access to food and water.
Ethics oversight	All animal procedures were approved and conducted in accordance with the guidelines of the Laboratory Animal Center (approval number: SUSTech-JY202201025-202402A1) at the Southern University of Science and Technology (SUSTech), Shenzhen.

Note that full information on the approval of the study protocol must also be provided in the manuscript.

Clinical data

Policy information about clinical studies

All manuscripts should comply with the ICMJE guidelines for publication of clinical research and a completed CONSORT checklist must be included with all submissions.

Clinical trial registration	*Provide the trial registration number from ClinicalTrials.gov or an equivalent agency.*

Study protocol	*Note where the full trial protocol can be accessed OR if not available, explain why.*
Data collection	*Describe the settings and locales of data collection, noting the time periods of recruitment and data collection.*
Outcomes	*Describe how you pre-defined primary and secondary outcome measures and how you assessed these measures.*

Dual use research of concern

Policy information about dual use research of concern

Hazards

Could the accidental, deliberate or reckless misuse of agents or technologies generated in the work, or the application of information presented in the manuscript, pose a threat to:

No	Yes	
☐	☐	Public health
☐	☐	National security
☐	☐	Crops and/or livestock
☐	☐	Ecosystems
☐	☐	Any other significant area

Experiments of concern

Does the work involve any of these experiments of concern:

No	Yes	
☐	☐	Demonstrate how to render a vaccine ineffective
☐	☐	Confer resistance to therapeutically useful antibiotics or antiviral agents
☐	☐	Enhance the virulence of a pathogen or render a nonpathogen virulent
☐	☐	Increase transmissibility of a pathogen
☐	☐	Alter the host range of a pathogen
☐	☐	Enable evasion of diagnostic/detection modalities
☐	☐	Enable the weaponization of a biological agent or toxin
☐	☐	Any other potentially harmful combination of experiments and agents

Plants

Seed stocks	*Report on the source of all seed stocks or other plant material used. If applicable, state the seed stock centre and catalogue number. If plant specimens were collected from the field, describe the collection location, date and sampling procedures.*
Novel plant genotypes	*Describe the methods by which all novel plant genotypes were produced. This includes those generated by transgenic approaches, gene editing, chemical/radiation-based mutagenesis and hybridization. For transgenic lines, describe the transformation method, the number of independent lines analyzed and the generation upon which experiments were performed. For gene-edited lines, describe the editor used, the endogenous sequence targeted for editing, the targeting guide RNA sequence (if applicable) and how the editor was applied.*
Authentication	*Describe any authentication procedures for each seed stock used or novel genotype generated. Describe any experiments used to assess the effect of a mutation and, where applicable, how potential secondary effects (e.g. second site T-DNA insertions, mosiacism, off-target gene editing) were examined.*

ChIP-seq

Data deposition

☐ Confirm that both raw and final processed data have been deposited in a public database such as GEO.

☐ Confirm that you have deposited or provided access to graph files (e.g. BED files) for the called peaks.

Data access links *May remain private before publication.*	*For "Initial submission" or "Revised version" documents, provide reviewer access links. For your "Final submission" document, provide a link to the deposited data.*
Files in database submission	*Provide a list of all files available in the database submission.*

Genome browser session
(e.g. UCSC)

Provide a link to an anonymized genome browser session for "Initial submission" and "Revised version" documents only, to enable peer review. Write "no longer applicable" for "Final submission" documents.

Methodology

Replicates

Describe the experimental replicates, specifying number, type and replicate agreement.

Sequencing depth

Describe the sequencing depth for each experiment, providing the total number of reads, uniquely mapped reads, length of reads and whether they were paired- or single-end.

Antibodies

Describe the antibodies used for the ChIP-seq experiments; as applicable, provide supplier name, catalog number, clone name, and lot number.

Peak calling parameters

Specify the command line program and parameters used for read mapping and peak calling, including the ChIP, control and index files used.

Data quality

Describe the methods used to ensure data quality in full detail, including how many peaks are at FDR 5% and above 5-fold enrichment.

Software

Describe the software used to collect and analyze the ChIP-seq data. For custom code that has been deposited into a community repository, provide accession details.

Flow Cytometry

Plots

Confirm that:

☐ The axis labels state the marker and fluorochrome used (e.g. CD4-FITC).

☐ The axis scales are clearly visible. Include numbers along axes only for bottom left plot of group (a 'group' is an analysis of identical markers).

☐ All plots are contour plots with outliers or pseudocolor plots.

☐ A numerical value for number of cells or percentage (with statistics) is provided.

Methodology

Sample preparation

Describe the sample preparation, detailing the biological source of the cells and any tissue processing steps used.

Instrument

Identify the instrument used for data collection, specifying make and model number.

Software

Describe the software used to collect and analyze the flow cytometry data. For custom code that has been deposited into a community repository, provide accession details.

Cell population abundance

Describe the abundance of the relevant cell populations within post-sort fractions, providing details on the purity of the samples and how it was determined.

Gating strategy

Describe the gating strategy used for all relevant experiments, specifying the preliminary FSC/SSC gates of the starting cell population, indicating where boundaries between "positive" and "negative" staining cell populations are defined.

☐ Tick this box to confirm that a figure exemplifying the gating strategy is provided in the Supplementary Information.

Magnetic resonance imaging

Experimental design

Design type

Indicate task or resting state; event-related or block design.

Design specifications

Specify the number of blocks, trials or experimental units per session and/or subject, and specify the length of each trial or block (if trials are blocked) and interval between trials.

Behavioral performance measures

State number and/or type of variables recorded (e.g. correct button press, response time) and what statistics were used to establish that the subjects were performing the task as expected (e.g. mean, range, and/or standard deviation across subjects).

Acquisition

Imaging type(s) *Specify: functional, structural, diffusion, perfusion.*

Field strength *Specify in Tesla*

Sequence & imaging parameters *Specify the pulse sequence type (gradient echo, spin echo, etc.), imaging type (EPI, spiral, etc.), field of view, matrix size, slice thickness, orientation and TE/TR/flip angle.*

Area of acquisition *State whether a whole brain scan was used OR define the area of acquisition, describing how the region was determined.*

Diffusion MRI ☐ Used ☐ Not used

Preprocessing

Preprocessing software *Provide detail on software version and revision number and on specific parameters (model/functions, brain extraction, segmentation, smoothing kernel size, etc.).*

Normalization *If data were normalized/standardized, describe the approach(es): specify linear or non-linear and define image types used for transformation OR indicate that data were not normalized and explain rationale for lack of normalization.*

Normalization template *Describe the template used for normalization/transformation, specifying subject space or group standardized space (e.g. original Talairach, MNI305, ICBM152) OR indicate that the data were not normalized.*

Noise and artifact removal *Describe your procedure(s) for artifact and structured noise removal, specifying motion parameters, tissue signals and physiological signals (heart rate, respiration).*

Volume censoring *Define your software and/or method and criteria for volume censoring, and state the extent of such censoring.*

Statistical modeling & inference

Model type and settings *Specify type (mass univariate, multivariate, RSA, predictive, etc.) and describe essential details of the model at the first and second levels (e.g. fixed, random or mixed effects; drift or auto-correlation).*

Effect(s) tested *Define precise effect in terms of the task or stimulus conditions instead of psychological concepts and indicate whether ANOVA or factorial designs were used.*

Specify type of analysis: ☐ Whole brain ☐ ROI-based ☐ Both

Statistic type for inference *Specify voxel-wise or cluster-wise and report all relevant parameters for cluster-wise methods.*

(See Eklund et al. 2016)

Correction *Describe the type of correction and how it is obtained for multiple comparisons (e.g. FWE, FDR, permutation or Monte Carlo).*

Models & analysis

n/a	Involved in the study
☐	☐ Functional and/or effective connectivity
☐	☐ Graph analysis
☐	☐ Multivariate modeling or predictive analysis

Functional and/or effective connectivity *Report the measures of dependence used and the model details (e.g. Pearson correlation, partial correlation, mutual information).*

Graph analysis *Report the dependent variable and connectivity measure, specifying weighted graph or binarized graph, subject- or group-level, and the global and/or node summaries used (e.g. clustering coefficient, efficiency, etc.).*

Multivariate modeling and predictive analysis *Specify independent variables, features extraction and dimension reduction, model, training and evaluation metrics.*